28 Eilken HM, Nishikawa S, Schroeder T. Continuous single-cell imaging of blood generation from haemogenic endothelium. *Nature* 2009; **457**: 896–900.
29 Red-Horse K, Crawford Y, Shojaei F, Ferrara N. Endothelium–microenvironment interactions in the developing embryo and in the adult. *Dev Cell* 2007; **12**: 181–94.
30 Asahara T, Murohara T, Sullivan A, Silver M, van der Zee R, Li T, Witzenbichler B, Schatteman G, Isner JM. Isolation of putative progenitor endothelial cells for angiogenesis. *Science* 1997; **275**: 964–7.
31 Purhonen S, Palm J, Rossi D, Kaskenpää N, Rajantie I, Ylä-Herttuala S, Alitalo K, Weissman IL, Salven P. Bone marrow-derived circulating endothelial precursors do not contribute to vascular endothelium and are not needed for tumor growth. *Proc Natl Acad Sci U S A* 2008; **105**: 6620–5.
32 Ferrara N. Vascular endothelial growth factor: basic science and clinical progress. *Endocr Rev* 2004; **25**: 581–611.
33 Takakura N, Watanabe T, Suenobu S, Yamada Y, Noda T, Ito Y, Satake M, Suda T. A role for hematopoietic stem cells in promoting angiogenesis. *Cell* 2000; **102**: 199–209.
34 Fukuhara S, Sako K, Minami T, Noda K, Kim HZ, Kodama T, Shibuya M, Takakura N, Koh GY, Mochizuki N. Differential function of Tie2 at cell-cell contacts and cell-substratum contacts regulated by angiopoietin-1. *Nat Cell Biol* 2008; **10**: 513–26.
35 Bellocq A, Antoine M, Flahault A, Philippe C, Crestani B, Bernaudin JF, Mayaud C, Milleron B, Baud L, Cadranel J. Neutrophil alveolitis in bronchioloalveolar carcinoma: induction by tumor derived interleukin-8 and relation to clinical outcome. *Am J Pathol* 1998; **152**: 83–92.
36 Coussens LM, Tinkle CL, Hanahan D, Werb Z. MMP-9 supplied by bone marrow-derived cells contributes to skin carcinogenesis. *Cell* 2000; **103**: 481–90.
37 Cassatella MA. Neutrophil-derived proteins: selling cytokines by the pound. *Adv Immunol* 1999; **73**: 369–509.
38 McCourt M, Wang JH, Sookhai S, Redmond HP. Proinflammatory mediators stimulate neutrophildirected angiogenesis. *Arch Surg* 1999; **134**: 1325–31.
39 Queen MM, Ryan RE, Holzer RG, Keller-Peck CR, Jorcyk CL. Breast cancer cells stimulate neutrophils to produce oncostatin M: potential implications for tumor progression. *Cancer Res* 2005; **65**: 8896–904.
40 Lin EY, Pollard JW. Role of infiltrated leucocytes in tumour growth and spread. *Br J Cancer* 2004; **90**: 2053–8.
41 Bergers G, Benjamin LE. Tumorigenesis and the angiogenic switch. *Nat Rev Cancer* 2003; **3**: 401–10.
42 Balkwill F, Charles KA, Mantovani A. Smoldering and polarized inflammation in the initiation and promotion of malignant disease. *Cancer Cell* 2005; **7**: 211–7.
43 De Palma M, Venneri MA, Galli R, Sergi Sergi L, Politi LS, Sampaolesi M, Naldini L. Tie-2 identifies a hematopoietic lineage of proangiogenic monocytes required for tumor vessel formation and a mesenchymal population of pericyte progenitors. *Cancer Cell* 2005; **8**: 211–26.
44 Ribatti D, Vacca A, Nico B, Crivellato E, Roncali L, Dammacco F. The role of mast cells in tumour angiogenesis. *Br J Haematol* 2001; **115**: 514–21.
45 Theoharides TC, Kempuraj D, Tagen M, Conti P, Kalogeromitros D. Differential release of mast cell mediators and the pathogenesis of inflammation. *Immunol Rev* 2007; **217**: 65–78.
46 Gabrilovich DI, Bronte V, Chen SH, Colombo MP, Ochoa A, Ostrand-Rosenberg S, Schreiber H. The terminology issue for myeloid-derived suppressor cells. *Cancer Res* 2007; **67**: 425.
47 Yang L, DeBusk LM, Fukuda K, Fingleton B, Green-Jarvis B, Shyr Y, Matrisian LM, Carbone DP, Lin PC. Expansion of myeloid immune suppressor Gr^+CD11b^+ cells in tumor-bearing host directly promotes tumor angiogenesis. *Cancer Cell* 2004; **6**: 409–21.
48 Puxeddu I, Alian A, Piliponsky AM, Ribatti D, Panet A, Levi-Schaffer F. Human peripheral blood eosinophils induce angiogenesis. *Int J Biochem Cell Biol* 2005; **37**: 628–36.
49 Curiel TJ, Cheng P, Mottram P, Alvarez X, Moons L, Evdemon-Hogan M, Wei S, Zou L, Kryczek I, Hoyle G, Lackner A, Carmeliet P, Zou W. Dendritic cell subsets differentially regulate angiogenesis in human ovarian cancer. *Cancer Res* 2004; **64**: 5535–8.
50 Scimone ML, Lutzky VP, Zittermann SI, Maffia P, Jancic C, Buzzola F, Issekutz AC, Chuluyan HE. Migration of polymorphonuclear leucocytes is influenced by dendritic cells. *Immunology* 2005; **114**: 375–85.
51 Conejo-Garcia JR, Buckanovich RJ, Benencia F, Courreges MC, Rubin SC, Carroll RG, Coukos G. Vascular leukocytes contribute to tumor vascularization. *Blood* 2005; **105**: 679–81.
52 Conejo-Garcia JR, Benencia F, Courreges MC, Kang E, Mohamed-Hadley A, Buckanovich RJ, Holtz DO, Jenkins A, Na H, Zhang L, Wagner DS, Katsaros D, Caroll R, Coukos G. Tumor-infiltrating dendritic cell precursors recruited by a b-defensin contribute to vasculogenesis under the influence of VEGF-A. *Nat Med* 2004; **10**: 950–8.
53 Fuchs E, Tumbar T, Guasch G. Socializing with the neighbors: stem cells and their niche. *Cell* 2004; **116**: 769–78.
54 Ottersbach K, Dzierzak E. The murine placenta contains hematopoietic stem cells within the vascular labyrinth region. *Dev Cell* 2005; **8**: 377–87.
55 Zhang J, Niu C, Ye L, Huang H, He X, Tong WG, Ross J, Haug J, Johnson T, Feng JQ, Harris S, Wiedemann LM, Mishina Y, Li L. Identification of the haematopoietic stem cell niche and control of the niche size. *Nature* 2003; **425**: 836–41.
56 Arai F, Hirao A, Ohmura M, Sato H, Matsuoka S, Takubo K, Ito K, Koh GY, Suda T. Tie2/angiopoietin-1 signaling regulates hematopoietic stem cell quiescence in the bone marrow niche. *Cell* 2004; **118**: 149–61.
57 Kiel MJ, Morrison SJ. Maintaining hematopoietic stem cells in the vascular niche. *Immunity* 2006; **25**: 862–4.
58 Sugiyama T, Kohara H, Noda M, Nagasawa T. Maintenance of the hematopoietic stem cell pool by CXCL12-CXCR4 chemokine signaling in bone marrow stromal cell niches. *Immunity* 2006; **25**: 977–88.
59 Li W, Johnson SA, Shelley WC, Ferkowicz M, Morrison P, Li Y, Yoder MC. Primary endothelial cells isolated from the yolk sac and para-aortic splanchnopleura support the expansion of adult marrow stem cells *in vitro*. *Blood* 2003; **102**: 4345–53.
60 Kobayashi H, Butler JM, O'Donnell R, Kobayashi M, Ding BS, Bonner B, Chiu VK, Nolan DJ, Shido K, Benjamin L, Rafii S. Angiocrine factors from Akt-activated endothelial cells balance self-renewal and differentiation of haematopoietic stem cells. *Nat Cell Biol* 2010; **12**: 1046–56.
61 Takakura N, Kodama H, Nishikawa S, Nishikawa S. Preferential proliferation of murine colony-forming units in culture in a chemically defined condition with a macrophage colony-stimulating factor-negative stromal cell clone. *J Exp Med* 1996; **184**: 2301–9.
62 Nikolova G, Strilic B, Lammert E. The vascular niche and its basement membrane. *Trends Cell Biol* 2007; **17**: 19–25.
63 Palmer TD, Willhoite AR, Gage FH. Vascular niche for adult hippocampal neurogenesis. *J Comp Neurol* 2000; **425**: 479–94.
64 Calabrese C, Poppleton H, Kocak M, Hogg TL, Fuller C, Hamner B, Oh EY, Gaber MW, Finklestein D, Allen M, Frank A, Bayazitov IT, Zakharenko SS, Gajjar A, Davidoff A, Gilbertson RJ. A perivascular niche for brain tumor stem cells. *Cancer Cell* 2007; **11**: 69–82.
65 Nagahama Y, Ueno M, Miyamoto S, Morii E, Minami T, Mochizuki N, Saya H, Takakura N. PSF1, a DNA replication factor expressed widely in stem and progenitor cells, drives tumorigenic and metastatic properties. *Cancer Res* 2010; **70**: 1215–24.
66 Butler JM, Kobayashi H, Rafii S. Instructive role of the vascular niche in promoting tumour growth and tissue repair by angiocrine factors. *Nat Rev Cancer* 2010; **10**: 138–46.

The American Journal of Pathology, Vol. 179, No. 6, December 2011

DOI: 10.1016/j.ajpath.2011.08.024

Short Communication

Apelin Attenuates UVB-Induced Edema and Inflammation by Promoting Vessel Function

Mika Sawane,* Hiroyasu Kidoya,† Fumitaka Muramatsu,† Nobuyuki Takakura,† and Kentaro Kajiya*

From the Shiseido Innovative Science Research Center, Yokohama; and the Department of Signal Transduction,† Research Institute of Microbial Diseases, Osaka University, Suita, Osaka, Japan*

Apelin, the ligand of the G protein–coupled receptor APJ, is involved in the regulation of cardiovascular functions, fluid homeostasis, and vessel formation. Recent reports indicate that apelin secreted from endothelial cells mediates APJ regulation of blood vessel caliber size; however, the function of apelin in lymphatic vessels is unclear. Here we report that APJ was expressed by human lymphatic endothelial cells and that apelin induced migration and cord formation of lymphatic endothelial cells dose-dependently *in vitro*. Furthermore, permeability assays demonstrated that apelin stabilizes lymphatic endothelial cells. *In vivo*, transgenic mice harboring apelin under the control of keratin 14 (K14-apelin) exhibited attenuated UVB-induced edema and a decreased number of CD11b-positive macrophages. Moreover, activation of apelin/APJ signaling inhibited UVB-induced enlargement of lymphatic and blood vessels. Finally, K14-apelin mice blocked the hyperpermeability of lymphatic vessels in inflamed skin. These results indicate that apelin plays a functional role in the stabilization of lymphatic vessels in inflamed tissues and that apelin might be a suitable target for prevention of UVB-induced inflammation. *(Am J Pathol 2011, 179:2691–2697; DOI: 10.1016/j.ajpath.2011.08.024)*

The lymphatic vascular system is composed of a dense network of thin-walled capillaries that drain protein-rich lymph from the extracellular space; its function is important for homeostasis of the circulatory and immune systems, maintenance of interstitial fluid composition and volume, and immune cell trafficking in health and in disease.[1,2] Chronic skin inflammation in mice has been associated with lymphatic endothelial cell (LEC) proliferation, and the skin disease psoriasis exhibited pronounced cutaneous lymphatic hyperplasia,[3] indicating that the lymphatic vascular system participates in both acute and chronic inflammation.

Acute exposure of skin to UVB irradiation (290 to 320 nm) leads to inflammation associated with epidermal hyperplasia, erythema, vascular hyperpermeability, and edema formation.[4,5] Previous studies have demonstrated that acute UVB irradiation of both human and mouse skin promotes marked angiogenesis.[6,7] Several angiogenesis factors, including vascular endothelial growth factor-A (VEGF-A), basic fibroblast growth factor, and interleukin-8, were up-regulated in skin after UVB-irradiation.[7–9] Thrombospondin-1, a potent endogenous angiogenesis inhibitor, was up-regulated.[7] Moreover, targeted overexpression of VEGF-A enhanced sensitivity to UVB-induced cutaneous photodamage,[10] but transgenic overexpression of thrombospondin-1 in the epidermis completely prevented UVB-induced photodamage.[11] Taken together, these findings indicate that the cutaneous blood vasculature plays an important role in the mediation of photodamage. A previous study from our research group demonstrated that UVB irradiation caused enlargement of lymphatic vessels with leaky and hyperpermeable function.[12] More recently, we found that activation of the VEGF-C/VEGFR-3 pathway attenuates UVB-induced inflammation by promoting lymphangiogenesis.[13] These studies point to a crucial role of lymphatic vessels in UVB-induced inflammation.

Apelin is an endogenous ligand for the previously orphan G protein–coupled receptor, APJ. The apelin gene (*APLN*), which is located on the long arm of the human X chromosome, encodes a 77-amino-acid preproprotein that is then cleaved to shorter active peptides.[14,15] The full-length mature peptide, which was originally isolated from bovine stomach extracts, comprises 36 amino acids and is known as apelin-36; the short-length peptide is known as apelin-13. Both peptides activate APJ.[16] APJ

Accepted for publication August 31, 2011.

M.S. and H.K. contributed equally to the present work.

Address reprint requests to Kentaro Kajiya, Ph.D., Shiseido Innovative Science Research Center, 2-12-1 Fukuura Kanazawa-ku, Yokohama 236-8643, Japan. E-mail: kentaro.kajiya@to.shiseido.co.jp.

expression has been reported in the cardiovascular system and in the central nervous system.[17,18] In the brain, the apelin/APJ system plays a role in maintaining body fluid homeostasis and regulating release of vasopressin from the hypothalamus.[19] In the cardiovascular system, APJ is expressed in endothelial cells, vascular smooth muscle cells, and cardiomyocytes.[20,21] Apelin/APJ in cells of endothelial lineage promotes hypotensive activity[22]; the activation of APJ leads to nitric oxide (NO) production by the endothelial cells,[23] and this possibly plays a role in the relaxation of smooth muscle cells.

Apelin is also essential for blood vessel formation. The apelin/APJ system plays a role in the cardiovascular system of *Xenopus laevis*[24] and of zebrafish.[25] *Xenopus* apelin (Xapelin) is expressed in the region around the presumptive blood vessels during early embryogenesis as *Xenopus* APJ (Xmsr). Knockdown of Xapelin or Xmsr resulted in a defect of blood vessel formation in the posterior cardinal vein, intersomitic vessels, and vitelline vessels. The regulation of blood vessel formation by apelin in mammals has been described recently. The Apelin/APJ system was shown to be involved in downstream signaling of Ang1/Tie2 in endothelial cells and in regulation of blood vessel diameter during angiogenesis.[26] However, the function of apelin in lymphatic vessels and its role in inflammation is not completely clear.

In the present study, we found that the APJ receptor is expressed in lymphatic endothelial cells *in vitro* and *in vivo*, and that apelin/APJ signaling promotes stabilization of lymphatic vessels. Moreover, using apelin transgenic mice, we demonstrated that apelin attenuates UVB-induced inflammation by promoting stabilization of lymphatic and blood vessels. These results suggest that apelin might be a suitable target for prevention of UVB-induced skin inflammation and photodamage.

Materials and Methods

Cells

Human dermal LECs were isolated from neonatal human foreskins by immunomagnetic purification, as described previously.[27] The lineage-specific differentiation was confirmed by real-time RT-PCR for the lymphatic vascular markers Prox1, LYVE-1, and podoplanin, as well as by immunostaining for Prox1 and podoplanin, as described previously.[28] Human umbilical vein endothelial cells (HUVECs) were purchased from PromoCell (Heidelberg, Germany). Cells were cultured in endothelial basal medium (Lonza, Verviers, Belgium) supplemented with supplements provided by the suppliers for up to 11 passages.

Immunoblotting

For Western blot analyses of APJ, Akt, and p-Akt, confluent LECs and HUVECs were homogenized in lysis buffer, and protein concentrations were determined using a DC protein assay kit (Bio-Rad Laboratories, Hercules, CA). Equal amounts of lysates (10 μg protein) were immunoblotted with a rabbit polyclonal antibody against APJ, as described previously.[26] LECs were also cultured with apelin-36 (1000 ng/mL; Peptide Institute, Osaka, Japan) for 2 minutes, followed by homogenization in lysis buffer. Untreated cells were prepared as controls in the same manner. Cell lysates (100 μg total protein each) were immunoprecipitated with antibodies against p-Akt and Akt (Cell Signaling Technology, Danvers, MA). Equal loading was confirmed with an antibody against β-actin (Sigma-Aldrich, St. Louis, MO).

Migration and Cord Formation Assays

The LEC migration assay was performed as described previously,[29] using 24-well FluoroBlock inserts of 8-μm pore size (Falcon; BD Biosciences, Franklin Lakes, NJ). The bottom sides of the inserts were coated with 10 μg/mL fibronectin (BD Biosciences, Bedford, MA) for 1 hour, followed by incubation with 100 μg/mL of bovine serum albumin. Cells (10^5 cells in 100 μL) were seeded in serum-free endothelial basal medium into the upper chambers, and were incubated for 5 hours at 37°C in the presence or absence of human recombinant apelin-13 (500 to 1000 ng/mL) or apelin-36 (500 to 1000 ng/mL). Cells on the underside of inserts were stained with Hoechst dye 33342 (Molecular Probes; Invitrogen, Carlsbad, CA). Five different digital images were captured per well, and the number of migrated cells was counted. Cord formation assays were performed as described previously.[30] LECs were grown on fibronectin-coated 24-well plates until confluence. In all, 0.5 mL of neutralized isotonic bovine dermal collagen type I (Vitrogen; Celtrix Laboratories, Palo Alto, CA) in the presence or absence of apelin-13 (50 to 1000 ng/mL) or apelin-36 (50 to 1000 ng/mL) was added to the cells. After incubation at 37°C for 24 hours, cells were fixed with 4% paraformaldehyde for 30 minutes at 4°C. Before lymphatic endothelial cells form tubes in collagen gels, endothelial cells connect with each other to make cords *in vitro*. Representative images were captured, and the total length of cordlike structures per area was measured using IP-LAB software version 4.0. All studies were performed in triplicate. Statistical analyses were performed using the unpaired Student's *t*-test.

Permeability Assay

LECs were grown into confluence on the fibronectin-coated surface of tissue culture inserts of 0.4-μm pore size (Transwell; Corning, Lowell, MA) and then in serum-free endothelial basal medium for 24 hours. Apelin-13 (500 to 1000 ng/mL) was placed into the upper and lower chambers for 6 hours. Fluorescein isothiocyanate-dextran was added to the upper chambers, and the apparatus was then placed in a CO_2 incubator at 37°C. After incubation for 15 minutes, a 100-μL sample was taken from the lower chamber, and the absorbance of fluorescein isothiocyanate-dextran was determined at 492 nm using a spectrophotometer (Fluoroskan Ascent; Thermo Fisher Scientific, Waltham, MA).

UVB Irradiation Regimen

Transgenic mice harboring apelin under the control of keratin 14 (K14-apelin) were generated on a C57BL/6 background, as described previously.[31] A total of 10 K14-apelin mice and wild-type (WT) mice, 12 weeks old (n = 5/group) were exposed to a single dose of 200 mJ/cm^2 of UVB irradiation using 10 Toshiba FL-20 SD fluorescent lamps that deliver energy in the UVB wavelength range (280 to 340 nm) with maximum energy at a wavelength of 305 nm. On day 3 or 4 after UVB irradiation, mouse ears were collected and were processed for histological analysis of frozen sections. Control mice without UVB irradiation were also analyzed. All procedures including UVB irradiation were performed under anesthesia. The study was approved by the ethics committee of Shiseido Research Center in accordance with guidelines of the U.S. National Institutes of Health (7th edition).

Intravital Lymphangiography and Plasma Extravasation

WT and K14-apelin mice (n = 5/group) were anesthetized with avertin (0.4 g/kg; Sigma-Aldrich), and 1 mL of a 1% solution of Evans Blue dye in 0.9% NaCl was injected intradermally at the inner surface of the rim of the ear, using a 10-mL Hamilton syringe, to visualize the lymphatic vessels. Mouse ears were photographed at 1 and 5 minutes after dye injection. To determine blood vascular permeability, a Miles assay was performed as described previously.[31] Briefly, mice were anesthetized and intravenously injected with 100 μL of a 1% solution of Evans Blue dye in 0.9% NaCl. At 60 minutes after dye injection, ears were photographed and then removed. The dye was eluted from the dissected samples with formamide at 56°C, and the optical density was measured by spectrophotometry (Biotrak II; GE Healthcare, Piscataway, NJ) at 620 nm.

Immunostaining and Computer-Assisted Morphometric Vessel Analysis

Immunofluorescence analysis was performed on cryostat sections (6 μm thick) of mouse ears using antibodies against the macrophage monocyte marker CD11b (Pharmingen; BD Biosciences, San Diego, CA), the blood vessel-specific marker Meca-32 (BD Biosciences), and the lymphatic-specific marker podoplanin (Acris Antibodies, Hiddenhausen, Germany) and using corresponding secondary antibodies labeled with Alexa Fluor 488 or Alexa Fluor 594 (Molecular Probes; Invitrogen). Routine H&E staining was also performed. Sections were examined with an Olympus AX80T microscope (Olympus, Tokyo, Japan), and images were captured with a DP controller digital camera (DP71; Olympus). Morphometric analyses were performed using IP-LAB software version 4.0, as described previously.[28] Three different fields of each section were examined, and ear thickness and the number of macrophages and average vessel size in the dermis were determined. Statistical analyses were performed using the unpaired Student's t-test.

Results

Apelin Is Expressed by Lymphatic Vessels both in Vitro *and* in Vivo *and Promotes Lymphatic Function*

To investigate whether apelin functions in lymphatic endothelial cells, we analyzed the expression of apelin receptor APJ in LECs. Western blot analyses demonstrated that APJ was expressed by both LECs and HUVECs (Figure 1A). Moreover, immunofluorescence analysis of mouse ear skin using antibodies against APJ and the blood vessel marker Meca-32 or the lymphatic marker podoplanin revealed that APJ was expressed by both lymphatic vessels (Figure 1C) and blood vessels (Figure 1B) *in vivo*. Apelin is known to activate the phosphorylation of Akt in HUVECs.[32] Treatment of LECs with 1000 ng/mL apelin-36 resulted in the increased phosphorylation of Akt, compared with untreated cells (Figure 1D). Migration assays performed to further characterize the effects of apelin on LEC revealed that both apelin-13 and apelin-36 induced LEC migration in a dose-dependent manner (Figure 1, E and F). To investigate whether apelin stimulation might promote cord formation of lymphatic endothelial cells *in vitro*, confluent LECs were overlaid with type I collagen. Cord formation of LECs was clearly enhanced in the presence of apelin-13 and apelin-36, compared with control cells (Figure 1, G–I). Morphometric analyses confirmed that both apelin-13 and apelin-36 induced cord formation of LECs dose-dependently ($P <$ 0.01) (Figure 1, J and K). A permeability assay was performed to determine whether apelin contributes to the stabilization of LECs *in vitro*. LECs were cultured on Transwell culture inserts into confluence, and the concentration of fluorescein isothiocyanate-dextran that permeated across the culture inserts was measured with or without apelin-13. The addition of 500 or 1000 ng/mL of apelin-13 in LECs decreased the fluorescence intensity of permeated fluorescein isothiocyanate-dextran, indicating that apelin promoted the stabilization of LECs ($P <$ 0.01) (Figure 1L).

Apelin Enhances Recovery from UVB-Induced Edema Formation and Inflammation

To determine the functional role of apelin in the cutaneous vasculature *in vivo*, transgenic mice harboring apelin under the control of keratin-14 (K14-apelin) and WT control mice were exposed to 200 mJ cm^{-2} of UVB irradiation. H&E staining of skin sections at 3 days after UVB irradiation revealed characteristic features of acute photodamage in the ear skin of WT mice, including epidermal hyperplasia and edema formation in the dermis (Figure 2C). Of note, K14-apelin mouse ears irradiated with UVB were closely similar to those of non-UVB-irradiated skin (Figure 2, A, B, and D). In a physiological condition, by contrast, no obvious difference was found between WT

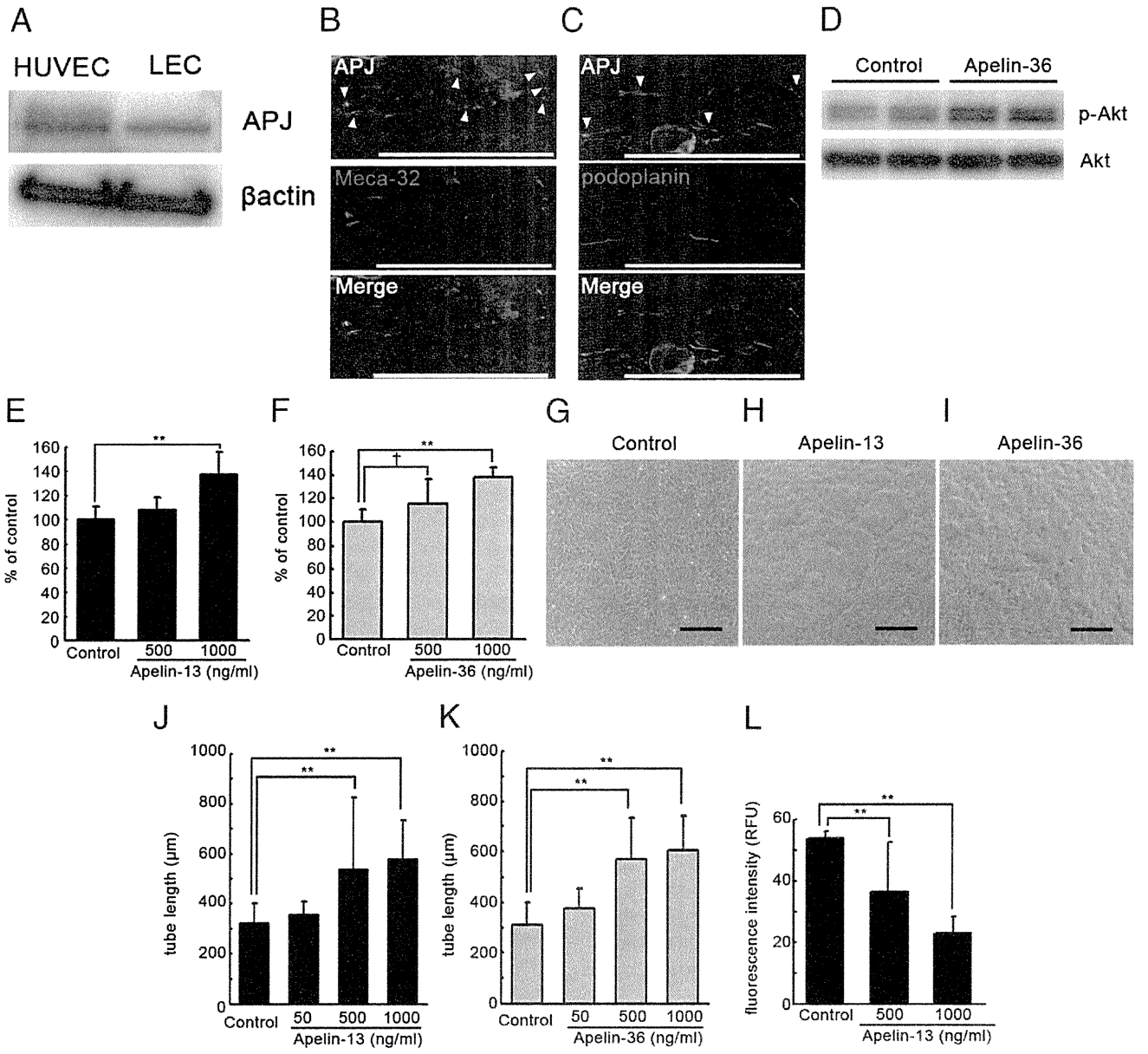

Figure 1. Apelin promotes formation and stabilization of lymphatic endothelial cells (LECs) *in vitro*. **A:** Immunoblot analyses confirmed that the apelin receptor APJ was expressed by both LECs and HUVECs. **B** and **C:** Double immunofluorescence analyses for APJ (green) and blood vessel marker Meca-32 (red, **B**) or lymphatic vessel marker podoplanin (red, **C**) revealed that APJ was expressed by both blood vessels and lymphatic vessels *in vivo*. **Arrowheads** show APJ expression in blood vessels (**B**) and lymphatic vessels (**C**). **D:** Treatment of LECs with 1000 ng/mL apelin-36 resulted in increased phosphorylation of Akt, compared with untreated cells. **E** and **F:** Apelin-13 (**E**) and apelin-36 (**F**) induced migration of LECs in a dose-dependent manner, compared with untreated control cells. **G–I:** Incubation of LECs with 500 ng/mL or 1000 ng/mL apelin-13 (**H** and **J**) and apelin-36 (**I** and **K**) enhanced cord formation in a dose-dependent manner after overlay with a type I collagen gel, compared with controls (**G**). Scale bars: 100 μm. **L:** The addition of 500 or 1000 ng/mL of apelin-13 decreased the fluorescence intensity of permeated fluorescein isothiocyanate-dextran from LEC, compared with controls. Data are expressed as means ± SD. $^{**}P < 0.01$; $^{\dagger}P < 0.1$.

and K14-apelin mice. The measurement of skin thickness confirmed that ear swelling was decreased in K14-apelin mouse ears, compared with WT mouse ears, after UVB irradiation ($P < 0.05$) (Figure 2I). Immunohistochemical staining for a monocyte macrophage marker, CD11b, demonstrated an increased number of infiltrating macrophages in the dermis of WT ears after UVB irradiation, compared with non-UVB-irradiated skin (Figure 2, E–G); however, the ear skin of UVB-irradiated K14-apelin mice exhibited decreased macrophage infiltration in the dermis (Figure 2H). Morphometric analyses confirmed a decreased number of infiltrating macrophages in the dermis of UVB-irradiated K14-apelin mouse ears, compared with WT mice after UVB-irradiation ($P < 0.01$) (Figure 2J).

Activation of Apelin/APJ Pathway Inhibits UVB-Induced Inflammation by Blocking Abnormal Enlargement of Lymphatic Vessels and Blood Vessels

To investigate how activation of apelin/APJ signaling attenuates edema formation and inflammation induced

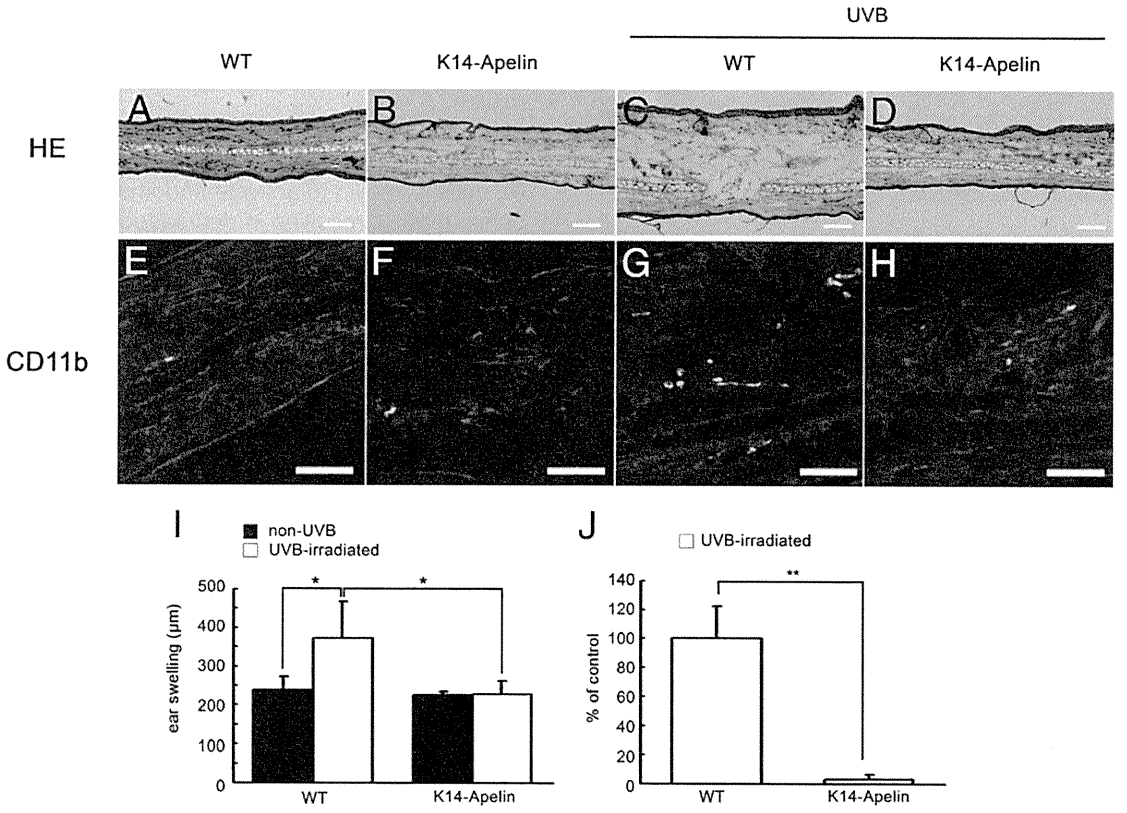

Figure 2. Apelin attenuates UVB-induced edema formation and inflammation. **A–D:** H&E staining revealed marked edema formation in the dermis of WT mouse ear skin (**C**), but K14-apelin mouse ear skin irradiated with UVB (**D**) was similar to non-UVB-irradiated skin (**A** and **B**). Scale bars: 100 μm. **E–H:** Immunofluorescence for CD11b (green) showed decreased macrophage infiltration in the dermis of K14-apelin mice ears (**H**), similar to non-UVB-irradiated mice (**E** and **F**), compared with WT mice irradiated with UVB (**G**). Scale bars: 100 μm. **I:** Skin thickness analysis indicated ear swelling in WT mice after UVB irradiation ($^*P < 0.05$), but this swelling was attenuated in K14-apelin mice. $^*P < 0.05$. **J:** The number of CD11b-positive cells was decreased in K14-apelin mice after UVB irradiation, compared with UVB-irradiated WT mice. $^{**}P < 0.01$. Morphometric analyses (**I** and **J**) were performed using IP-LAB software version 4.0. Data are expressed as mean values ± SD ($n = 3$).

by UVB irradiation, we analyzed cutaneous lymphatic vessels after UVB irradiation. To visualize lymphatic vessels, Evans Blue dye was injected intradermally into the rim of mouse ears. At 1 and 5 minutes after injection, Evans Blue dye had extravasated from lymphatic vessels in UVB-irradiated WT skin, but such leakage was attenuated in K14-apelin mice (Figure 3, A–D). Next, Miles assay was performed to determine the effects of apelin on blood vessels. UVB exposure induced marked leakage of Evans Blue dye in WT mice (Figure 3E), but such leakage was attenuated in K14-apelin mice (Figure 3F). Quantitative analysis demonstrated that the increase of dye leakage in WT mouse ears was significantly blocked in UVB-irradiated K14-apelin mice (Figure 3G).

We performed double immunofluorescence staining for the lymphatic marker podoplanin and the blood vascular marker Meca-32. In a physiological condition, the density of blood vessels was similar between WT and K14-apelin mice, but K14-apelin mice exhibited increased size of blood vessels, as has been demonstrated previously.[31] No great difference in lymphatic vessel formation was immediately evident in K14-apelin mice; however, precise histological examination of skin stained for podoplanin revealed enlarged lymphatic vessels of K14-apelin mice, compared with WT mice (Figure 3, H–M). Enlargement of lymphatic vessels and blood vessels was induced in WT mice after UVB irradiation; surprisingly, however, in K14-apelin mice the UVB-induced enlargement of lymphatic and blood vessels was inhibited (Figure 3, N–S). Morphometric analyses of sections demonstrated that the average size of lymphatic vessels and blood vessels was significantly decreased in skin of UVB-irradiated K14-apelin mice, compared with WT mice after UVB-irradiation (−74%, $P < 0.05$ for lymphatic vessels; −26%, $P < 0.05$ for blood vessels; Figure 3, T and U).

Discussion

Apelin has been recently reported to be an important regulator of blood vessel formation. The present study reveals, for the first time, that the apelin receptor APJ is expressed by human lymphatic endothelial cells and that apelin/APJ signaling plays a crucial role in UVB-induced inflammation through stabilization of blood and lymphatic vessels.

Acute photodamage of the skin is characterized by epidermal hyperplasia, erythema, and edema formation. Edema is caused by accumulation of extracellular fluid due to excess leakage from hyperpermeable blood vessels[33] and by a failure of lymphatic vessels to sufficiently drain the fluid from the interstitium.[12] Moreover, the dys-

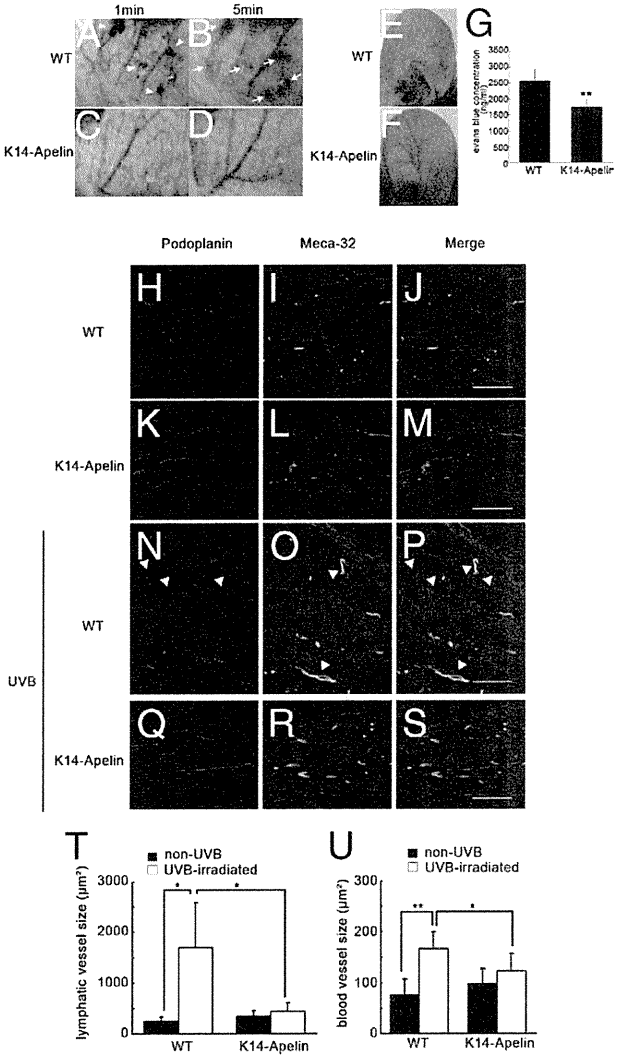

Figure 3. Activation of apelin/APJ signaling inhibited UVB-induced inflammation by blocking enlargement of lymphatic vessels and blood vessels. **A–D:** Evans Blue dye was injected intradermally into the rim of mouse ears. After 5 minutes, Evans Blue dye had extravasated from lymphatic vessels in UVB-irradiated WT mouse skin (**A**, **arrowheads**; **B**, **arrows**), but such leakage was attenuated in K14-apelin mice after UVB (**C** and **D**). **E–G:** Miles assay revealed that UVB exposure induced vascular hyperpermeability of WT mice (**E**), but this effect was markedly inhibited in K14-apelin mice (**F**). **G:** Quantitative analysis demonstrated increased Evans Blue leakage in the ear of UVB-irradiated WT mice, compared with UVB-irradiated K14-apelin mice. $^{**}P < 0.01$. **H–S:** Double immunofluorescence staining of ear sections for podoplanin (red) and Meca-32 (green) revealed enlargement (**arrowheads**) of podoplanin-positive lymphatic vessels and Meca-32-positive blood vessels in UVB-irradiated WT mice (**N–P**), compared with nonirradiated mice (**H–M**). This enlargement of lymphatic vessels and blood vessels after UVB irradiation was blocked in K14-apelin mice (**Q–S**). Scale bars: 100 μm. **T** and **U:** According to morphometric analyses using IP-LAB software version 4.0, the average size of lymphatic vessels (**T**) and blood vessels (**U**) was significantly reduced in K14-apelin mice after UVB irradiation ($^{*}P < 0.05$). In contrast, size of lymphatic vessels and blood vessels was increased in WT mice irradiated with UVB. $^{*}P < 0.05$; $^{**}P < 0.01$.

function of lymphatic vessels also results in reduced clearance of macrophages from the tissue via lymphatic drainage,[34] suggesting that the function of lymphatic vessels is profoundly related to the process of UVB-induced inflammation. We have previously reported that skin tissues during days 2 to 4 after UVB irradiation exhibit enlargement of lymphatic vessels and macrophage infiltration.[13] Surprisingly, K14-apelin mice inhibited the enlargement and hyperpermeability of lymphatic vessels and macrophage infiltration by UVB irradiation, indicating that apelin plays a defensive role in UVB-induced inflammation.

How does apelin attenuate skin inflammation? Although the function of the apelin/APJ system in endothelial cells is known to activate endothelial nitric oxide synthase (eNOS), resulting in decreased the blood pressure with vasodilation,[22] the present results indicate that apelin attenuates the abnormal enlargement of lymphatic and blood vessels in inflamed skin. Additionally, plasma extravasation was markedly decreased in K14-apelin mice, compared with WT mice after UVB irradiation, indicating a protective role of apelin in blood vessels, as described recently.[31] Moreover, we have previously demonstrated that systemic blockade of lymphatic function by the VEGFR-3 pathway prolongs UVB-induced edema formation and inflammation,[35] whereas intradermal injection of VEGF-C accelerates the resolution of UVB-induced edema and inflammation by inducing lymphangiogenesis.[13] In contrast to such VEGF-C treatment, no major differences in the number of lymphatic vessels were observed in skin of K14-apelin mice. It was therefore of considerable interest to see the differential mechanism of attenuating inflammation by apelin. A previous study from our research group demonstrated that acute UVB irradiation increases overextension of lymphatic vessels, which leads to impaired fluid transport and so contributes to prolonged edema formation.[12] Of note, the hyperpermeability of lymphatic vessels was blocked in K14-apelin mice after UVB irradiation, compared with that observed in UVB-irradiated WT mice, and the permeability assay *in vitro* demonstrated that apelin blocked the permeability of human lymphatic endothelial cells. Taken together, these data suggest that inhibiting hyperpermeability by enhancing apelin expression could facilitate transport of tissue fluid, resulting in rapid resolution of edema and the related inflammation induced by UVB.

The molecular events that regulate blood vessel formation, especially the caliber size determination of blood vessels by apelin, have been recently suggested. A remarkable study showed that the apelin/APJ system is involved in downstream signaling of Ang1/Tie2 in blood vessel formation.[26] With the present study, we have demonstrated that apelin induces migration and cord formation of LECs and that lymphatic vascular size in K14-apelin mice is greater than in WT mice. Given that apelin induces expression of the junctional proteins claudin-5 and vascular endothelial cadherin (VE-cadherin) in blood vessels, resulting in abundant cell-to-cell contact and regulation of endothelial cell assembly, it is possible that apelin inhibits hyperpermeability of lymphatic vessels and inflammation by UVB-irradiation via the regulation of the junctional protein in lymphatic endothelial cells.[26] Further studies would be needed to clarify a molecular regulation of lymphatic integrity by apelin and to determine whether apelin is involved in downstream Ang1/Tie2 signaling in lymphatic vessels.

In summary, the present results indicate that apelin plays a functional role in the stabilization of lymphatic vessels in inflamed tissues. Apelin might be a new

suitable target for prevention of UVB-induced skin inflammation.

Acknowledgment

We thank Fumika Miyohashi for her technical assistance.

References

1. Cueni LN, Detmar M: New insights into the molecular control of the lymphatic vascular system and its role in disease. J Invest Dermatol 2006, 126:2167–2177
2. Tammela T, Alitalo K: Lymphangiogenesis: molecular mechanisms and future promise. Cell 2010, 140:460–476
3. Kunstfeld R, Hirakawa S, Hong YK, Schacht V, Lange-Asschenfeldt B, Velasco P, Lin C, Fiebiger E, Wei X, Wu Y, Hicklin D, Bohlen P, Detmar M: Induction of cutaneous delayed-type hypersensitivity reactions in VEGF-A transgenic mice results in chronic skin inflammation associated with persistent lymphatic hyperplasia. Blood 2004, 104:1048–1057
4. Kligman AM: The treatment of photoaged human skin by topical tretinoin. Drugs 1989, 38:1–8
5. Kripke ML: Ultraviolet radiation and immunology: something new under the sun—presidential address. Cancer Res 1994, 54:6102–6105
6. Yano K, Kadoya K, Kajiya K, Hong YK, Detmar M: Ultraviolet B irradiation of human skin induces an angiogenic switch that is mediated by upregulation of vascular endothelial growth factor and by downregulation of thrombospondin-1. Br J Dermatol 2005, 152:115–121
7. Yano K, Kajiya K, Ishiwata M, Hong YK, Miyakawa T, Detmar M: Ultraviolet B-induced skin angiogenesis is associated with a switch in the balance of vascular endothelial growth factor and thrombospondin-1 expression. J Invest Dermatol 2004, 122:201–208
8. Krämer M, Sachsenmaier C, Herrlich P, Rahmsdorf HJ: UV irradiation-induced interleukin-1 and basic fibroblast growth factor synthesis and release mediate part of the UV response. J Biol Chem 1993, 268:6734–6741
9. Strickland I, Rhodes LE, Flanagan BF, Friedmann PS: TNF-alpha and IL-8 are upregulated in the epidermis of normal human skin after UVB exposure: correlation with neutrophil accumulation and E-selectin expression. J Invest Dermatol 1997, 108:763–768
10. Hirakawa S, Fujii S, Kajiya K, Yano K, Detmar M: Vascular endothelial growth factor promotes sensitivity to ultraviolet B-induced cutaneous photodamage. Blood 2005, 105:2392–2399
11. Yano K, Oura H, Detmar M: Targeted overexpression of the angiogenesis inhibitor thrombospondin-1 in the epidermis of transgenic mice prevents ultraviolet-B-induced angiogenesis and cutaneous photo-damage. J Invest Dermatol 2002, 118:800–805
12. Kajiya K, Hirakawa S, Detmar M: Vascular endothelial growth factor-a mediates ultraviolet B-induced impairment of lymphatic vessel function. Am J Pathol 2006, 169:1496–1503
13. Kajiya K, Sawane M, Huggenberger R, Detmar M: Activation of the VEGFR-3 pathway by VEGF-C attenuates UVB-induced edema formation and skin inflammation by promoting lymphangiogenesis. J Invest Dermatol 2009, 129:1292–1298
14. Hosoya M, Kawamata Y, Fukusumi S, Fujii R, Habata Y, Hinuma S, Kitada C, Honda S, Kurokawa T, Onda H, Nishimura O, Fujino M: Molecular and functional characteristics of APJ. Tissue distribution of mRNA and interaction with the endogenous ligand apelin. J Biol Chem 2000, 275:21061–21067
15. Tatemoto K, Hosoya M, Habata Y, Fujii R, Kakegawa T, Zou MX, Kawamata Y, Fukusumi S, Hinuma S, Kitada C, Kurokawa T, Onda H, Fujino M: Isolation and characterization of a novel endogenous peptide ligand for the human APJ receptor. Biochem Biophys Res Commun 1998, 251:471–476
16. Masri B, Knibiehler B, Audigier Y: Apelin signalling: a promising pathway from cloning to pharmacology. Cell Signal 2005, 17:415–426
17. Devic E, Rizzoti K, Bodin S, Knibiehler B, Audigier Y: Amino acid sequence and embryonic expression of msr/apj, the mouse homolog of Xenopus X-msr and human APJ. Mech Dev 1999, 84:199–203
18. O'Dowd BF, Heiber M, Chan A, Heng HH, Tsui LC, Kennedy JL, Shi X, Petronis A, George SR, Nguyen T: A human gene that shows identity with the gene encoding the angiotensin receptor is located on chromosome 11. Gene 1993, 136:355–360
19. De Mota N, Reaux-Le Goazigo A, El Messari S, Chartrel N, Roesch D, Dujardin C, Kordon C, Vaudry H, Moos F, Llorens-Cortes C: Apelin, a potent diuretic neuropeptide counteracting vasopressin actions through inhibition of vasopressin neuron activity and vasopressin release. Proc Natl Acad Sci USA 2004, 101:10464–10469
20. Devic E, Paquereau L, Vernier P, Knibiehler B, Audigier Y: Expression of a new G protein-coupled receptor X-msr is associated with an endothelial lineage in Xenopus laevis. Mech Dev 1996, 59:129–140
21. Katugampola SD, Maguire JJ, Matthewson SR, Davenport AP: [(125)I]-(Pyr(1))Apelin-13 is a novel radioligand for localizing the APJ orphan receptor in human and rat tissues with evidence for a vasoconstrictor role in man. Br J Pharmacol 2001, 132:1255–1260
22. Ishida J, Hashimoto T, Hashimoto Y, Nishiwaki S, Iguchi T, Harada S, Sugaya T, Matsuzaki H, Yamamoto R, Shiota N, Okunishi H, Kihara M, Umemura S, Sugiyama F, Yagami K, Kasuya Y, Mochizuki N, Fukamizu A: Regulatory roles for APJ, a seven-transmembrane receptor related to angiotensin-type 1 receptor in blood pressure in vivo. J Biol Chem 2004, 279:26274–26279
23. Tatemoto K, Takayama K, Zou MX, Kumaki I, Zhang W, Kumano K, Fujimiya M: The novel peptide apelin lowers blood pressure via a nitric oxide-dependent mechanism. Regul Pept 2001, 99:87–92
24. Cox CM, D'Agostino SL, Miller MK, Heimark RL, Krieg PA: Apelin, the ligand for the endothelial G-protein-coupled receptor, APJ, is a potent angiogenic factor required for normal vascular development of the frog embryo. Dev Biol 2006, 296:177–189
25. Scott IC, Masri B, D'Amico LA, Jin SW, Jungblut B, Wehman AM, Baier H, Audigier Y, Stainier DY: The G protein-coupled receptor Agtrl1b regulates early development of myocardial progenitors. Dev Cell 2007, 12:403–413
26. Kidoya H, Ueno M, Yamada Y, Mochizuki N, Nakata M, Yano T, Fujii R, Takakura N: Spatial and temporal role of the apelin/APJ system in the caliber size regulation of blood vessels during angiogenesis. EMBO J 2008, 27:522–534
27. Hirakawa S, Hong YK, Harvey N, Schacht V, Matsuda K, Libermann T, Detmar M: Identification of vascular lineage-specific genes by transcriptional profiling of isolated blood vascular and lymphatic endothelial cells. Am J Pathol 2003, 162:575–586
28. Kajiya K, Hirakawa S, Ma B, Drinnenberg I, Detmar M: Hepatocyte growth factor promotes lymphatic vessel formation and function. EMBO J 2005, 24:2885–2895
29. Hong YK, Lange-Asschenfeldt B, Velasco P, Hirakawa S, Kunstfeld R, Brown LF, Bohlen P, Senger DR, Detmar M: VEGF-A promotes tissue repair-associated lymphatic vessel formation via VEGFR-2 and the alpha1beta1 and alpha2beta1 integrins. FASEB J 2004, 18:1111–1113
30. Kajiya K, Huggenberger R, Drinnenberg I, Ma B, Detmar M: Nitric oxide mediates lymphatic vessel activation via soluble guanylate cyclase alpha1beta1: impact on inflammation. FASEB J 2008, 22:530–537
31. Kidoya H, Naito H, Takakura N: Apelin induces enlarged and nonleaky blood vessels for functional recovery from ischemia. Blood 2010, 115:3166–3174
32. Masri B, Morin N, Pedebernade L, Knibiehler B, Audigier Y: The apelin receptor is coupled to Gi1 or Gi2 protein and is differentially desensitized by apelin fragments. J Biol Chem 2006, 281:18317–18326
33. Persson CG: Role of plasma exudation in asthmatic airways. Lancet 1986, 2:1126–1129
34. Kataru RP, Jung K, Jang C, Yang H, Schwendener RA, Baik JE, Han SH, Alitalo K, Koh GY: Critical role of CD11b+ macrophages and VEGF in inflammatory lymphangiogenesis, antigen clearance, and inflammation resolution. Blood 2009, 113:5650–5659
35. Kajiya K, Detmar M: An important role of lymphatic vessels in the control of UVB-induced edema formation and inflammation. J Invest Dermatol 2006, 126:919–921

Biochemical and Biophysical Research Communications 415 (2011) 174–180

Contents lists available at SciVerse ScienceDirect

Biochemical and Biophysical Research Communications

journal homepage: www.elsevier.com/locate/ybbrc

2-Methoxycinnamaldehyde inhibits tumor angiogenesis by suppressing Tie2 activation

Daishi Yamakawa [a], Hiroyasu Kidoya [a], Susumu Sakimoto [a], Weizhen Jia [a], Nobuyuki Takakura [a,b,*]

[a] Department of Signal Transduction, Research Institute for Microbial Diseases, Osaka University, 3-1 Yamada-oka, Suita-shi, Osaka 565-0871, Japan
[b] JST, CREST, Sanbancho, Chiyoda-ku, Tokyo 102-0075, Japan

ARTICLE INFO

Article history:
Received 20 September 2011
Available online 18 October 2011

Keywords:
2-Methoxycinnamaldehyde
Tie2
Angiopoietin-1
Angiogenesis

ABSTRACT

Blood vessels are mainly composed of intraluminal endothelial cells (ECs) and mural cells adhering to the ECs on their basal side. Immature blood vessels lacking mural cells are leaky; thus, the process of mural cell adhesion to ECs is indispensable for stability of the vessels during physiological angiogenesis. However, in the tumor microenvironment, although some blood vessels are well-matured, the majority is immature. Because mural cell adhesion to ECs also has a marked anti-apoptotic effect, angiogenesis inhibitors that destroy immature blood vessels may not affect mature vessels showing more resistance to apoptosis. Activation of Tie2 receptor tyrosine kinase expressed in ECs mediates pro-angiogenic effects via the induction of EC migration but also facilitates vessel maturation via the promotion of cell adhesion between mural cells and ECs. Therefore, inhibition of Tie2 has the advantage of completely inhibiting angiogenesis. Here, we isolated a novel small molecule Tie2 kinase inhibitor, identified as 2-methoxycinnamaldehyde (2-MCA). We found that 2-MCA inhibits both sprouting angiogenesis and maturation of blood vessels, resulting in inhibition of tumor growth. Our results suggest a potent clinical benefit of disrupting these two using Tie2 inhibitors.

1. Introduction

It is well-established that dysregulation of blood vessel formation is involved in several diseases, such as cancer, retinopathy, chronic inflammation and others. To develop optimal strategies for inhibiting angiogenesis and preventing progression of these diseases, the mechanisms controlling blood vessel formation have been extensively analyzed. Of the many growth factors involved in this process, vascular endothelial growth factor (VEGF) or its cognate receptors (VEGFRs) have been targeted by angiogenesis inhibitors which are already utilized clinically, especially in cancer therapy [1]. Indeed, the efficacy of neutralizing antibody to VEGF (bevacizumab) in prolonging survival in patients with malignant colon cancer has been established, and utilization of this drug is currently being extended to other tumor types [2].

VEGF plays a fundamental role in development, tube formation and proliferation of endothelial cells (ECs) [3]. Tubes generated using VEGF alone do not mature; blood vessel stability requires the adherence of mural cells such as pericytes or smooth muscle cells to ECs on the basal side. When Tie2, a receptor tyrosine kinase, expressed predominantly in ECs, is activated by angiopoietin-1 (Ang1), usually released from mural cells, cell adhesion between ECs and mural cells is induced and the structural stability of blood vessels is enhanced [4]. It is widely accepted that mural cell adhesion to ECs induces a transition from the actively elongating status of a new blood vessel to a mature state, resulting in finalization of sprouting angiogenesis. On the other hand, when angiogenesis is ongoing and mural cells are absent near ECs, Tie2 activation induces migration of ECs to support sprouting angiogenesis. Therefore, Tie2 activation plays dual roles as a pro-angiogenic and as an anti-angiogenic factor. Which activity dominates is dependent on intracellular signaling via Tie2 phosphorylation [5]. When it is mainly the Akt pathway that is activated through Tie2, cell adhesion between mural cells and ECs is induced, resulting in vascular quiescence. However, when the Erk rather than Akt pathway is activated via Tie2, the migration of ECs is enhanced.

In the context of therapy with angiogenesis inhibitors, maturation of blood vessels is a key locus for the development of resistance against angiogenesis inhibitors. Mural cells adhere to ECs in mature blood vessels. In this situation, the two cell types engage in cross-talk and stimulate each other by producing several cytokines such as VEGF, Ang1, platelet-derived growth factor (PDGF), transforming growth factor β and others [6]. This results in suppression of apoptosis of both mural cells and ECs. Moreover,

Abbreviations: 2-MCA, 2-methoxycinnamaldehyde; EC, endothelial cell; Ang1, angiopoietin-1; VEGF, vascular endothelial growth factor.

* Corresponding author at: Department of Signal Transduction, Research Institute for Microbial Diseases, Osaka University, 3-1 Yamada-oka, Suita-shi, Osaka 565-0871, Japan. Fax: +81 6879 8314.
E-mail address: ntakaku@biken.osaka-u.ac.jp (N. Takakura).

0006-291X/$ - see front matter © 2011 Elsevier Inc. All rights reserved.
doi:10.1016/j.bbrc.2011.10.053

adhesion molecules responsible for keeping the mural cells and ECs in close proximity also provide signals involved in preventing their apoptosis. Tie2- or Ang1-deficient mice lack EC/mural cell integrity and manifest insufficient vessel outgrowth [7]. Therefore, Tie2 inhibition in tumors may suppress sprouting angiogenesis as well as inhibiting blood vessel maturation.

In the present study, we screened for small molecule Tie2 inhibitors in natural products. Among the molecules investigated, we found that 2-methoxycinnamaldehyde [(2E)-3-(2-methoxyphenyl)acrylaldehyde: 2-MCA] inhibits Ang1-mediated Tie2 phosphorylation. 2-MCA is extracted from the bark of cinnamon trees and other species of the genus *Cinnamomum* and gives those plants their flavor [8]. 2-MCA has been identified as the major active fungitoxic component, especially against Candida albicans [9], and also possesses strong antibacterial activity [10]. Here, we show that 2-MCA abrogates Ang1-mediated endothelial barrier function and tube formation in vitro. Moreover, using 2-MCA we analyzed whether Tie2 inhibition suppresses both the process of sprouting angiogenesis as well as blood vessel maturation in the tumor microenvironment.

2. Materials and methods

2.1. Screen for Tie2 kinase inhibitors

Human Tie2, cytoplasmic domain [771-1124(end) aminoacids was expressed as an N-terminal GST-fusion protein. First, we selected extracts from several herbs because of their inhibitory effects on proliferation or migration of ECs in the P-Sp culture system that supports vasculogenesis and angiogenesis [11]. Approximately 100 test compounds were isolated from extracts of these herbs by high performance liquid chromatography were evaluated. Compound solution, substrate/ATP/Metal solution, and kinase solution were prepared with assay buffer (15 mM Tris–HCl, 0.01% Tween-20, 2 mM DTT, pH 7.5) and mixed in streptavidin coated 96 well microplates (Perkin Elmer). Plates were incubated for 1 h at room temperature and then washed four times to stop the reaction. Wells were blocked with blocking buffer containing 0.1% BSA and then the detection antibody (HRP-conjugated PY20; Santa Cruz Biotechnology) was added and incubated for 30 min. After washing, TMB solution (MOSS, Inc.) was added to each well and incubated for 5 min. To stop the HRP reaction, 0.1 M sulfuric acid was added. The kinase reaction was evaluated by absorbance at 450 nm. Among compounds tested, we found one with Tie2 kinase inhibitory effects. This compound was identified as 2-MCA by NMR (NM-ECP400; JOEL).

2.2. Reagents

2-MCA (Sigma Aldrich), Recombinant human $VEGF_{165}$ (PEPROTECH), Ang1, and HGF (R&D Systems) were used.

In Western blotting analysis, mouse anti-Tie2 (Ab33) antibodies (Abs) (Upstate), phospho-Tie2 (Tyr992) (R&D Systems, Inc.), rabbit anti-Akt, phospho-Akt (Ser473), p44/42, phospho-p44/42 (Thr202/Tyr204) (Cell Signaling Technology, Inc.) and mouse anti-GAPDH mAb (Chemicon) were used as the first Abs. Anti-phosphoTie2 (Tyr992) Abs were diluted 1:500, other Abs 1:1000. HRP-conjugated anti-rabbit and anti-mouse Ig (Jackson ImmunoResearch) was used as the secondary antibody (diluted 1:1000).

For the immunofluorescence analysis, mouse anti-human ZO-1 (BD Biosciences), rat anti-mouse CD31 (BD Biosciences) and Cy3-conjugated anti-α-smooth muscle actin (1A4; Sigma) mAbs were used as the first Abs (diluted 1:200). Alexa488-conjugated goat anti-mouse and anti-rat Igs (Invitrogen) were used as the secondary Abs (Invitrogen) (dilution; 1:200).

2.3. Cell culture

Ba/F3 cells were grown in RPMI-1640 medium supplemented with 10% FBS and 200 pg/ml IL-3 (GIBCO). Human umbilical vein endothelial cells (HUVECs) were purchased from Kurabo (Kurashiki, Japan) and maintained according to the suppliers instructions. For Ang1, VEGF and HGF stimulation, cells were starved in RPMI-1640 medium containing 1% FBS for 3 h. Colon26 cells were grown in Dulbecco's modified Eagle's medium (DMEM) supplemented with 10% FBS. HCT116 cells were grown in RPMI-1640 medium supplemented with 10% FBS. Platinum-E cells (Plat-E; packaging cells) and stable cell lines transfected with pMRX virus vector were cultured in 10% FBS-containing DMEM [12,13].

2.4. Plasmid construction

Mouse Tie2 or mutant Tie2 (Tie2R848W) was fused to sequences encoding full-length Venus. A Myc epitope was inserted as a tag between Tie2 and Venus. Genes were inserted at the multicloning site of pEGFPN1 vector or pMRX virus vectors.

2.5. Retroviral infection

Plat-E cells were transfected with 1.0 μg of pMRX-Tie2-Myc-Venus or pMRX-Tie2R848W-Myc-Venus vectors using Lipofectamine 2000 (Invitrogen), then incubated for 24 h at 37 °C after which the medium was changed. After 12 h (36 h from transfection) and 24 h (48 h from transfection), conditioned medium was harvested, sterilized by filtration and used to infect Ba/F3 cells. About 8 μg/ml polybrene was added to facilitate infection. Stable cell lines expressing wild-type Tie2 (BaF/WT-Tie2 cells) or constitutively active Tie2 (BaF/R848W-Tie2 cells) were selected by culture in medium containing puromycin (5 μg/ml) or blasticidin (10 μg/ml).

2.6. SDS–PAGE and Western blotting

Cells were washed with ice-cold phosphate-buffered saline (PBS) and lyzed with RIPA buffer (50 mM Tris–HCl pH 7.5, 150 mM NaCl, 1% NP-40, 0.5% sodium deoxycholate, 0.1% SDS). The cells were incubated on ice for 10 min followed by centrifugation at 15,000 rpm for 5 min at 4 °C. Proteins electrophoretically separated using 7.5% SDS gels were transferred to nylon membranes (Amersham Biosciences) by a wet blotting procedure (140 V, 200 mA, 120 min). The membrane was blocked with 5% skim milk/TBST for 60 min, subsequently incubated with the Abs as indicated in the figures and processed for chemiluminescence detection with ECL solution.

2.7. Tube formation

HUVECs were cultured at 3×10^4 cells/well on 100 μl of growth factor-reduced Matrigel (BD Biosciences) in RPMI-1640 supplemented with 1% FBS. The cells were incubated for 18 h at 37 °C, 5% CO_2. Tube formation was observed in living cells microscopically (Leica AF6000).

2.8. Analysis of cell apoptosis

HUVECs were cultured for 24 h in the presence or absence of 2-MCA (30 μM). The cells were stained with Annexin V and propidium iodide using an Annexin V-FITC apoptosis detection kit (BD Biosciences), and analyzed by flow cytometry (Becton Dickinson).

2.9. Mice

Balb/c and KSN nude mice were purchased from Japan SLC (Shizuoka, Japan). Mouse and human colon cancer-derived colon26 and HCT116 cells (3.5×10^6 cells) were inoculated subcutaneously into 8 week-old female mice. Animals were housed in environmentally controlled rooms of the animal experimentation facility at Osaka University. All experiments were carried out following the guidelines of Osaka University Committee for animal and recombinant DNA experiments.

2.10. Immunocytochemistry and immunohistochemistry

For immunocytochemistry, cells on 0.1% gelatin (Sigma Aldrich)-coated glass dishes were rinsed, fixed for 10 min in 4% paraformaldehyde-PBS (pH 7.5) and washed with PBS. Subsequently, the cells were permeabilized with 0.1% Triton X-100 for 30 min. After washing with PBS, cells were blocked with PBS containing 5% normal goat serum and 1% BSA for 30 min and immunostained with first Abs (1:100) for 1 h. Protein reacting with Abs was visualized with secondary Abs (1:200). The cells were observed under a microscope (Leica TCS SP5 Ver1.6) using HCX PL APO lambda blue 63×1.4 oil. Images were processed using Adobe Photoshop CS5 Extended software (Adobe Systems). Immunohistochemical analysis was performed as previously reported [14].

2.11. Statistical analysis

Results were expressed as the mean ± SEM. Student's t test was used for statistical analysis. Differences were considered statistically significant when $P < 0.01$.

3. Results

3.1. 2-MCA inhibits phosphorylation of Tie2

Using an ELISA-based in vitro kinase assay to screen for Tie2 inhibitors, we identified 2-MCA as a novel candidate molecule. To confirm that 2-MCA inhibits Ang1-mediated Tie2 phosphorylation, a pro-B lymphocyte cell line (Ba/F3) expressing mouse Tie2 ectopically (BaF/WT-Tie2 cells) was used. When BaF/WT-Tie2 cells were stimulated with Ang1, phosphorylation of Tie2 was observed; this was suppressed by 2-MCA in a dose-dependent manner (Fig. 1A).

It is well known that Tie2 phosphorylation induces activation of downstream signal pathways such as PI3K-Akt and p42/44, Erk. We found that 2-MCA inhibited both of these Ang-1-stimulated, Tie2-dependent signaling cascades (Fig. 1B).

It has been reported that exchange of tryptophan for arginine at position 849 (R849W) of Tie2 by point mutation leads to its constitutive activation and that this mutation is one cause of human hereditary venous malformation [15]. We generated a construct

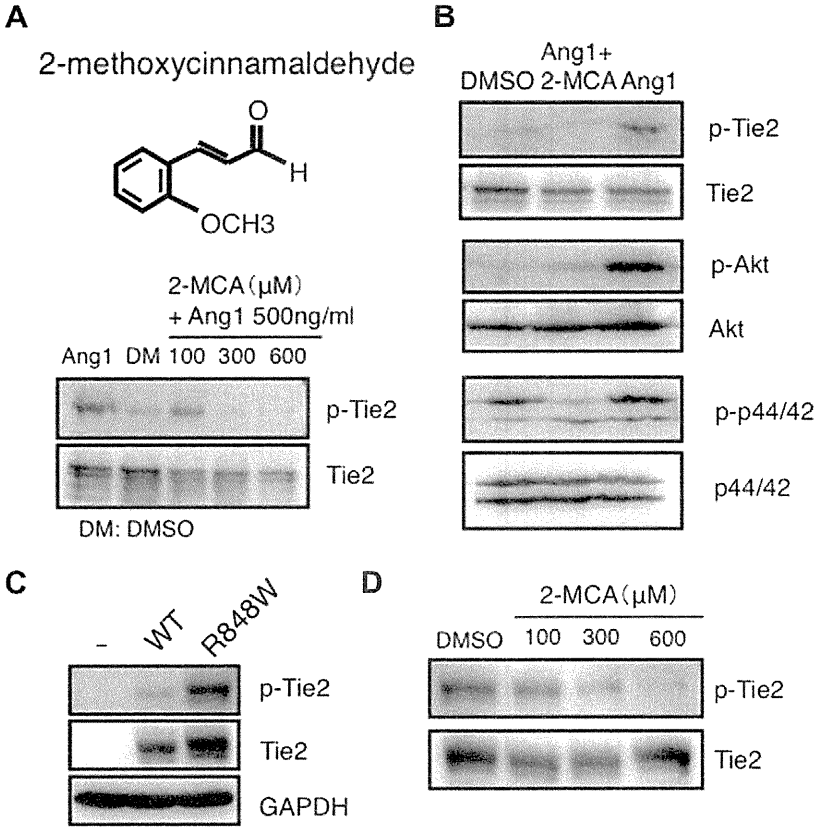

Fig. 1. 2-MCA inhibits phosphorylation of Tie2. (A) Chemical structural formula of 2-methoxycinnamaldehyde (2-MCA) (upper). Western blotting was performed using BaF/WT-Tie2 cells (bottom). BaF/WT-Tie2 cells were stimulated with or without Ang1 for 15 min in the presence or absence of titrated doses of 2-MCA. (B) Effect of 2-MCA on downstream signals of Tie2. BaF/WT-Tie2 cells were stimulated with or without Ang1 (500 ng/ml) for 15 min in the presence or absence of 2-MCA (600 μM). Phosphorylation of Tie2, Akt and p44/42 was assessed. (C) Western blotting of Ba/F3, BaF/WT-Tie2 (WT), and BaF/R848W-Tie2 cells (R848W). GAPDH was used as the internal control. (D) Inhibitory effect of 2-MCA on phosphorylation of constitutively active Tie2. BaF/R848W-Tie2 cells were cultured with titrated doses of 2-MCA as indicated for 15 min. Tie2 phosphorylation was then assessed.

coding for this mutant Tie2 in mice (R848W) and transfected it into Ba/F3 cells. Wild-type Tie2 was only weakly phosphorylated without Ang1 on overexpression, but mutant Tie2 was strongly phosphorylated (Fig. 1C). This phosphorylation of constitutively active Tie2 was also inhibited by 2-MCA in a dose-dependent manner (Fig. 1D).

3.2. 2-MCA inhibits Ang1-mediated stabilization of cell-cell junctions and tube formation

Activation of Tie2 in ECs enhances the stability of blood vessels and supports angiogenesis mainly via Akt or Erk activation, respectively, as described above [5]. Therefore, we next investigated whether 2-MCA affects these functions of Tie2 using human umbilical vein endothelial cells (HUVECs). We confirmed that activation of Akt and Erk mediated by stimulation with Ang1 was abrogated by 2-MCA in HUVECs (Fig. 2A), as was observed using BaF/Tie2 cells. When HUVECs reach confluence, tight junctions marked by ZO-1 appear (Fig. 2B). ZO-1 expression was not observed on EC–EC contact on stimulation with VEGF, consistent with its well known action to disturb EC–EC junction formation and facilitate hyperpermeability [16]. However, Ang1 inhibited VEGF-mediated disruption of junction formation. When 2-MCA was added at the same time as VEGF and Ang1, the effect of Ang1 on stabilization of EC-EC contact was annulled (Fig. 2B). This finding suggested that 2-MCA blocks maturation processes during blood vessel formation. When HUVECs were cultured on the Matrigels, Ang1 was seen to induce cord-like structures involved in tube formation, as previously reported [17] (Fig. 2C). However, 2-MCA suppressed this, consistent with its inhibitory effects on angiogenesis.

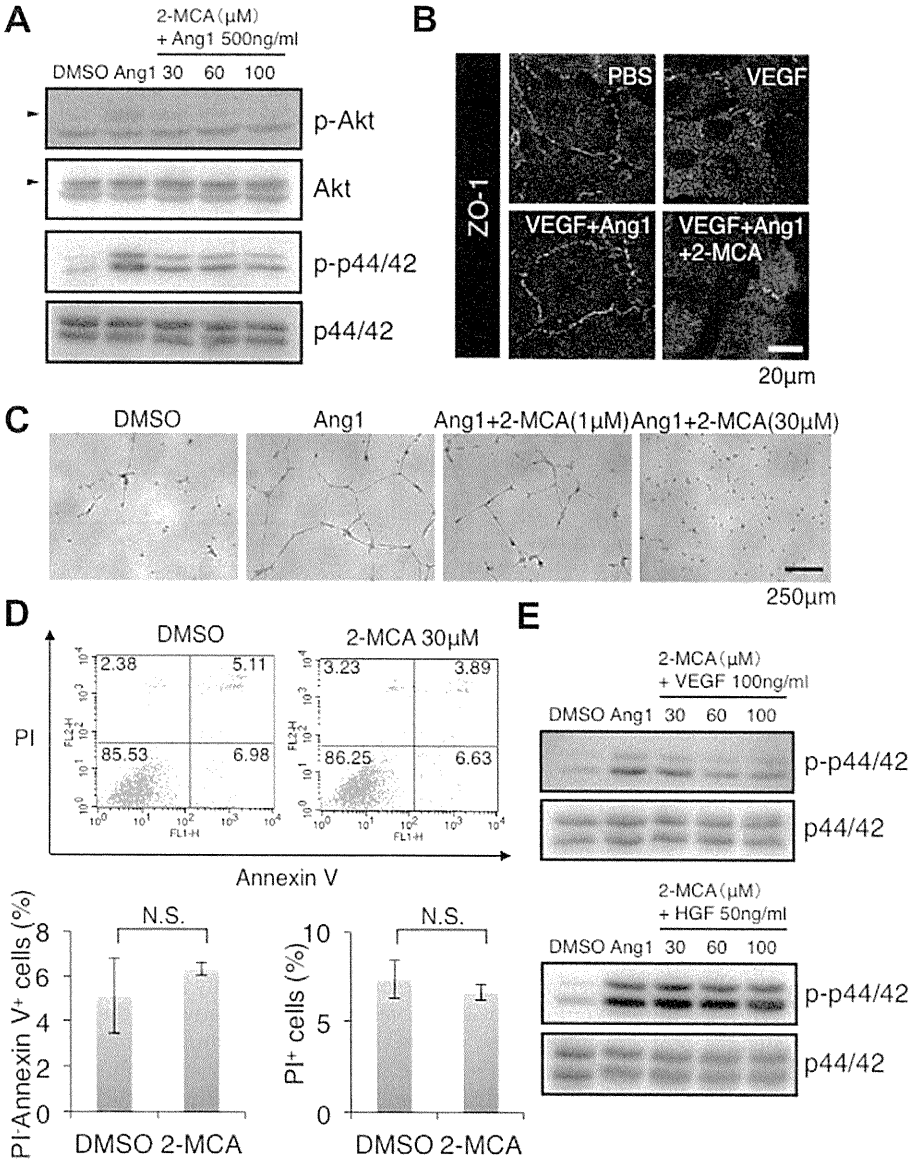

Fig. 2. Effects of 2-MCA on Ang1-mediated HUVEC junction and tube formation. (A) Effect of 2-MCA on Ang1-mediated Tie2 downstream signals, Akt and p42/44 in HUVECs. HUVECs were cultured with or without Ang1 (500 ng/ml) in the presence of titrated doses of 2-MCA as indicated for 15 min. (B) Effect of 2-MCA on Ang1-mediated membrane stability of the tight junction protein ZO-1. HUVECs were cultured with VEGF (10 ng/ml) with or without Ang1 (100 ng/ml) in the presence or absence of 2-MCA (60 μM) for 24 h, after which ZO-1 expression was assessed immunocytochemically. The bar indicates 20 μm. (C) Tube formation analysis. HUVECs were cultured on Matrigels with or without of Ang1 (500 ng/ml) in the presence or absence of titrated doses of 2-MCA as indicated. Bar indicates 250 μm. (D) HUVECs were cultured in the presence or absence of 2-MCA (30 μM) for 24 h and cell death and apoptosis was then evaluated by the expression of Annexin V and PI staining by FACS (upper). Numbers in each quadrant indicate the percentage of cells among total cells. Quantitative evaluation of $PI^-AnnexinV^+$ apoptotic cells and PI^+ dead cells (lower two graphs) ($n = 3$). (E) Effect of 2-MCA on VEGF- or HGF-mediated p42/44 activation in HUVECs. HUVECs were cultured for 15 min. with or without VEGF (100 ng/ml) or HGF (50 ng/ml) in the presence of titrated doses of 2-MCA as indicated.

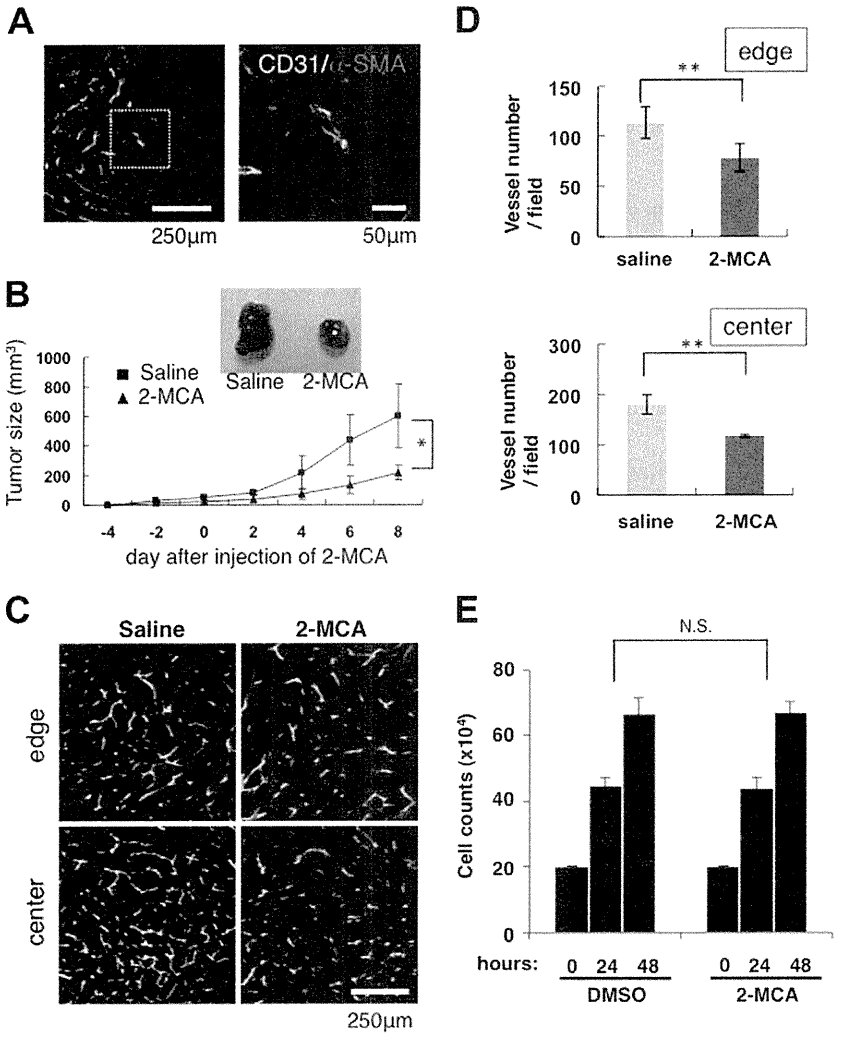

Fig. 3. Effect of 2-MCA on tumor angiogenesis. (A) Blood vessel formation observed in tumors established by inoculating colon26 mouse colon cancer cells. Section of tumor was stained with anti-CD31 (green) and anti-α-SMA (red) antibodies. Right panel shows higher magnification of area indicated by dashed box in the left panel. Bars indicate 250 μm (left) and 50 μm (right). (B) Effect of 2-MCA on tumor growth. 2-MCA (0.5 mg/kg) was injected intraperitoneally every day from day 0 to day 7, starting 4 days after inoculation of tumor cells. Tumor growth was monitored by measuring tumor size. Inset shows gross appearance of tumors dissected on day 8. $^{*}P < 0.05$ ($n = 3$). (C) Suppression of the formation of tumor vasculature by injecting 2-MCA. Sections from the edge and center lesions of the tumor were stained with anti-CD31 antibody. Bar indicates 250 μm. (D) Quantitative evaluation of vascular density calculated for the edge (upper) and center (bottom) of the tumor. The number of blood vessels in 5 random fields was counted. $^{**}P < 0.01$. (E) In vitro proliferation assay using colon26 cells with DMSO or 30 μM 2-MCA.

To investigate direct effects of 2-MCA on ECs, HUVECs were cultured in its presence or absence. Results suggested that the effects of 2-MCA did not depend on enhancement of HUVEC death or apoptosis (Fig. 2D). To further investigate whether the inhibitory effects of 2-MCA were mediated specifically via the angiopoietin/Tie2 pathway, cellular assays were performed to monitor Erk activation by two other angiogenesis-related receptor tyrosine kinases, VEGFR and c-Met, induced by their cognate ligands, VEGF and HGF, respectively. Similar to the results from stimulation by Ang1, both VEGF and HGF were capable of inducing the phosphorylation of Erk. However, no inhibitory effects of 2-MCA were observed on Erk activation by these factors (Fig. 2E). These results indicate that the observed effect of 2-MCA was most likely mediated through specific inhibition of the Ang1-triggered Tie2 activation pathway.

3.3. 2-MCA suppresses tumor growth via inhibition of angiogenesis

Using tumor xenograft models, we previously reported that there are two types of tumor associations with mural cell coverage of ECs in the tumor vasculature [14]. In one type, most blood vessels are not covered with mural cells and greater numbers of vessels develop in the tumor microenvironment. In the other type, mature blood vessels in which ECs are covered with mural cells are observed especially at the edge of the tumor, and the number of vessels is low relative to the first type. We have now tested the effect of 2-MCA on tumor angiogenesis in the first type using the mouse colon cancer cell line, colon26. As shown in Fig. 3A, blood vessels covered with mural cells are rare and angiogenesis is robustly induced in this tumor. Four days after cell inoculation into mice, we started to inject 2-MCA daily for 8 days and monitored tumor growth by evaluating tumor volume. The results documented a clear tumor growth inhibitory action of 2-MCA (Fig. 3B). Blood vessel formation was evaluated by dividing the area into edge and center of tumor; vascular density was found to be decreased in both areas (Fig. 3C and D). 2-MCA did not show any suppressive effects on proliferation of colon26 cells themselves in vitro (Fig. 3E). These data suggest that 2-MCA inhibited tumor growth by suppressing tumor angiogenesis.

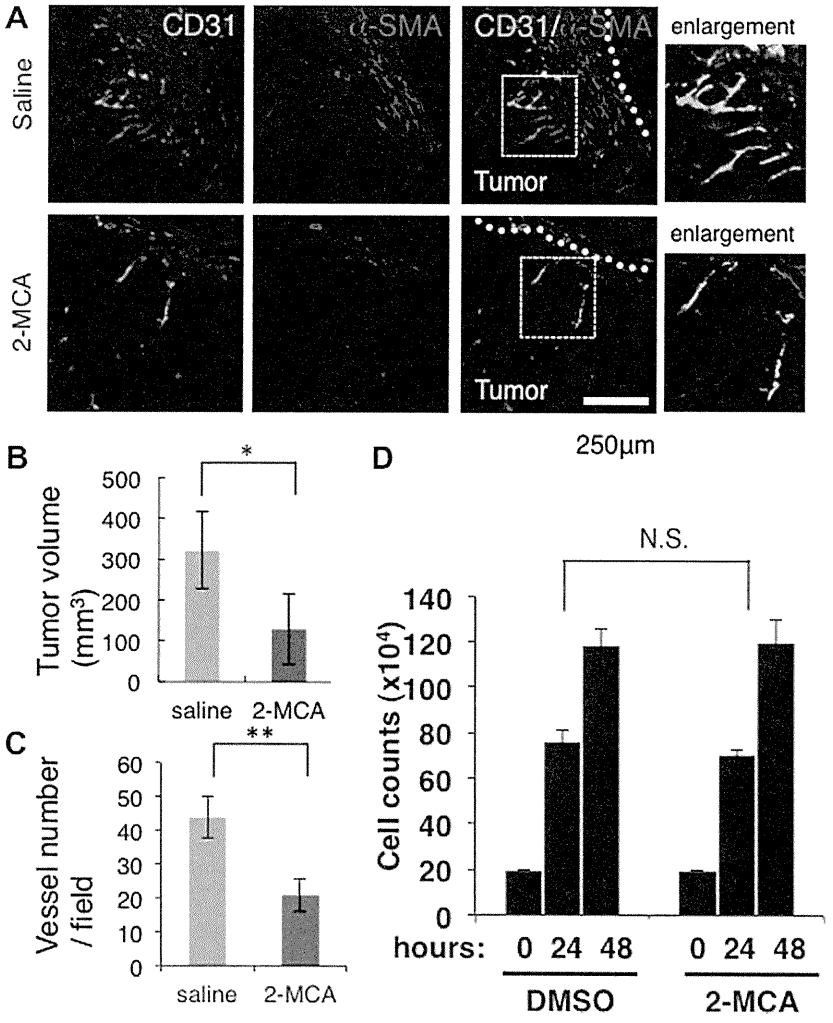

Fig. 4. Effect of 2-MCA on tumor angiogenesis. (A) Blood vessel formation observed in tumors established by inoculation of HCT116 human colon cancer cells. Schedule and doses of 2-MCA were the same as in Fig. 3. Tumors were dissected on day 8 (12 days after tumor cell inoculation) and sections were stained with anti-CD31 (green) and anti-α-SMA (red) antibodies. Right panels show higher magnification of area indicated by dashed box in the left-hand side. Bars indicate 250 μm. (B) Effect of 2-MCA on tumor growth. $^{*}P < 0.05$ ($n = 3$). (C) Quantitative evaluation of vascular density. The number of blood vessels in 5 random fields was counted. $^{**}P < 0.01$. (D) In vitro proliferation assay using HCT116 cells with DMSO or 30 μM 2-MCA.

3.4. 2-MCA inhibits maturation of the tumor vasculature

Using the human colon cancer cell line HCT116 in a xenograft model, we observed very few blood vessels in the center of the tumor but mature vessels covered with mural cells were plentiful at the periphery (Fig. 4A). To investigate whether 2-MCA affects maturation of blood vessels in the tumor environment, we injected it using the same schedule as described in Fig. 3B. Twelve days inoculation of tumor cells, the tumor volume was significantly smaller in the 2-MCA-injected group than in controls (Fig. 4B). Moreover, vascular density was also significantly reduced in the 2-MCA-injected group (Fig. 4A and C). The number of mature blood vessels that were still present in 2-MCA-treated tumors was reduced. 2-MCA did not mediate any direct suppressive effects on HCT116 cell proliferation in vitro (Fig. 4D). These data suggest that 2-MCA affects the maturation of blood vessels by inhibiting mural cell attachment.

4. Discussion

In this work, we screened natural products for Tie2 inhibitory activity and isolated 2-MCA, a small molecule which inhibited tumor growth by suppressing tumor angiogenesis. We cannot completely exclude the possibility that 2-MCA also affected angiogenesis by mechanisms other than Tie2 inhibition, but the finding that 2-MCA blocked Ang1-mediated tube formation and barrier formation implies that its inhibitory action on Tie2 must be at least partly responsible for its suppression of tumor angiogenesis.

One of the objectives of the present study was to identify inhibitors that can block maturation of blood vessels as well as progression of sprouting angiogenesis. This aim arose from the evidence that tumor repopulation is observed from the edge of the tumor even under circumstances where tumor growth seemed to be completely inhibited by treatment with vascular disrupting agents [18]. Similar evidence was also reported that invasion of cancer cells is induced from the edge of the tumor after treatment with angiogenesis inhibitors [19]. We previously reported that blood vessels are fully mature at the edge of the tumor, unlike in its center [14]. Therefore, invasion of cancer cells and repopulation of the tumor after treatment with angiogenesis inhibitors seems to be caused by the resistance of mature blood vessels in the tumor rim to the action of anti-angiogenic drugs. In our present studies using HT116 cells, the number of mature blood vessels in which ECs were covered with mural cells at the edge of the tumor was

reduced by 2-MCA treatment. Therefore, this agent is useful for inhibiting maturation processes of the tumor vasculature during tumor growth.

Constitutively active mutant Tie2 is seen in patients with hereditary venous malformation [15]. Recently, it has been reported that Tie2 constitutively active due to somatic mutation is also found in sporadic venous malformation [20]. Histopathological examination revealed that blood vessels are dilated in a disorderly manner and mural cell attachment is essentially absent in vascular lesions of such patients. Akt activation via Tie2 activation induces maturation of blood vessels. On the other hand, Erk activation via Tie2 activation induces angiogenesis. In the patients with constitutively active Tie2, it is likely that the Erk pathway is strongly activated. As reported here, 2-MCA could inhibit both Erk as well as Akt activation through Tie2 phosphorylation. Therefore, agents like 2-MCA should also be effective for treating lesions in venous malformation as well as tumor angiogenesis.

In terms of Tie2 inhibition, several lines of evidence from studies using soluble Tie2 receptors or aptamers have already suggested that Tie2 inhibition could be effective for suppressing tumor growth [21–23]. However, there is little data on using small molecule Tie2 inhibitors to prevent tumor growth. Although many kinase inhibitors for the VEGF receptor pathway have been developed, Tie2 inhibitors still require more developmental work for expansion of their application to different therapeutic approaches.

Acknowledgments

We thank N. Fujimoto, C. Takeshita for technical assistance. This work was partly supported by the Japanese Ministry of Education, Culture, Sports, Science and Technology, and the Japan Society for Promotion of Science.

References

[1] S.P. Ivy, J.Y. Wick, B.M. Kaufman, An overview of small-molecule inhibitors of VEGFR signaling, Nat. Rev. Clin. Oncol. 6 (2009) 569–579.
[2] H. Hurwitz, L. Fehrenbacher, W. Novotny, et al., Bevacizumab plus irinotecan, fluorouracil, and leucovorin for metastatic colorectal cancer, N. Engl. J. Med. 350 (2004) 2335–2342.
[3] N. Ferrara, H.P. Gerber, J. LeCouter, The biology of VEGF and its receptors, Nat. Med. 9 (2003) 669–676.
[4] H.G. Augustin, G.Y. Koh, G. Thurston, K. Alitalo, Control of vascular morphogenesis and homeostasis through the angiopoietin-Tie system, Nat. Rev. Mol. Cell Biol. 10 (2009) 165–177.
[5] S. Fukuhara, K. Sako, T. Minami, K. Noda, H.Z. Kim, T. Kodama, M. Shibuya, N. Takakura, G.Y. Koh, N. Mochizuki, Differential function of Tie2 at cell-cell contacts and cell-substratum contacts regulated by angiopoietin-1, Nat. Cell Biol. 10 (2008) 513–526.
[6] R.K. Jain, Molecular regulation of vessel maturation, Nat. Med. 9 (2003) 685–693.
[7] D.J. Dumont, G. Gradwohl, G.H. Fong, M.C. Puri, M. Gerstenstein, A. Auerbach, M.L. Breitman, Dominant-negative and targeted null mutations in the endothelial receptor tyrosine kinase, tek, reveal a critical role in vasculogenesis of the embryo, Genes Dev. 8 (1994) 1897–1909.
[8] S. Morozumi, Isolation purification and antibiotic activity of *o*-methoxycinnamaldehyde from *Cinnamon*, Appl. Environ. Microbiol. 36 (1978) 577–583.
[9] H.B. Singh, M. Srivastava, A.B. Singh, A.K. Srivastava, Cinnamon bark oil a potent fungitoxicant against fungi causing respiratory tract mycoses, Allergy 50 (1995) 995–999.
[10] S.T. Chang, P.F. Chen, S.C. Chang, Antibacterial activity of leaf essential oils and their constituents from *Cinnamomum osmophloeum*, J. Ethnopharmacol. 77 (2001) 123–127.
[11] N. Takakura, T. Watanabe, S. Suenobu, Y. Yamada, T. Noda, Y. Ito, M. Satake, T. Suda, A role for hematopoietic stem cells in promoting angiogenesis, Cell 102 (2000) 199–209.
[12] S. Morita, T. Kojima, T. Kitamura, Plat-E: an efficient and stable system for transient packaging of retroviruses, Gene Ther. 7 (2000) 1063–1066.
[13] T. Saitoh, H. Nakano, N. Yamamoto, S. Yamaoka, Lymphotoxin-L receptor mediates NEMO-independent NF-UB activation, FEBS Lett. 532 (2002) 45–51.
[14] N. Satoh, Y. Yamada, Y. Kinugasa, N. Takakura, Angiopoietin-1 alters tumor growth by stabilizing blood vessels or by promoting angiogenesis, Cancer Sci. 99 (2008) 2373–2379.
[15] M. Vikkula, L.M. Boon, K.L. Carraway, J.T. Calvert, A.J. Diamonti, B. Goumnerov, K.A. Pasyk, D.A. Marchuk, M.L. Warman, L.C. Cantley, J.B. Mulliken, B.R. Olsen, Vascular dysmorphogenesis caused by an activating mutation in the receptor tyrosine kinase TIE2, Cell 87 (1996) 1181–1190.
[16] S.W. Lee, W.J. Kim, Y.K. Choi, H.S. Song, M.J. Son, I.H. Gelman, Y.J. Kim, K.W. Kim, SSeCKS regulates angiogenesis and tight junction formation in blood-brain barrier, Nat. Med. 9 (2003) 900–906.
[17] I. Kim, H.G. Kim, S.O. Moon, S.W. Chae, J.N. So, K.N. Koh, B.C. Ahn, G.Y. Koh, Angiopoietin-1 induces endothelial cell sprouting through the activation of focal adhesion kinase and plasmin secretion, Cir. Res. 86 (2000) 952–959.
[18] G.M. Tozer, C. Kanthou, B.C. Baguley, Disrupting tumour blood vessels, Nat. Rev. Cancer 5 (2005) 423–435.
[19] M.P. Ribes, E. Allen, J. Hudock, T. Takeda, H. Okuyama, F. Vinals, M. Inoue, G. Bergers, D. Hanahan, O. Casanovas, Antiangiogenic therapy elicits malignant progression of tumors to increased local invasion and distant metastasis, Cancer Cell 15 (2009) 220–231.
[20] N. Limaye, V. Wouters, M. Uebelhoer, M. Tuominen, R. Wirkkala, J.B. Mulliken, L. Eklund, L.M. Boon, M. Vikkula, Somatic mutations in angiopoietin receptor gene TEK cause solitary and multiple sporadic venous malformations, Nat. Genet. 41 (2009) 118–124.
[21] P. Lin, P. Polverini, M. Dewhirst, S. Shan, P.S. Rao, K. Peters, Inhibition of tumor angiogenesis using a soluble receptor establishes a role for Tie2 in pathologic vascular growth, J. Clin. Invest. 100 (1997) 2072–2078.
[22] R. Tournaire, M.P. Simon, F.l. Noble, A. Eichmann, P. England, J. Pouyssegur, A short synthetic peptide inhibits signal transduction, migration and angiogenesis mediated by Tie2 receptor, EMBO Rep. 5 (2004) 262–267.
[23] Y.J. Koh, H.Z. Kim, S.I. Hwang, J.E. Lee, N. Oh, K. Jung, M. Kim, K.E. Kim, H. Kim, N.K. Lim, C.J. Jeon, G.M. Lee, B.H. Jeon, D.H. Nam, H.K. Sung, A. Nagy, O.J. Yoo, G.Y. Koh, Double antiangiogenic protein, DAAP, targeting VEGF-A and angiopoietins in tumor angiogenesis, metastasis, and vascular leakage, Cancer Cell 18 (2010) 171–184.

The American Journal of Pathology, Vol. 180, No. 3, March 2012

DOI: 10.1016/j.ajpath.2011.11.008

Vascular Biology, Atherosclerosis, and Endothelium Biology

Promotion of Lymphatic Integrity by Angiopoietin-1/Tie2 Signaling during Inflammation

Kentaro Kajiya,* Hiroyasu Kidoya,† Mika Sawane,* Yuuko Matsumoto-Okazaki,* Haruyo Yamanishi,* Mikio Furuse,‡ and Nobuyuki Takakura†

From the Shiseido Innovative Science Research Center, Yokohama; the Department of Signal Transduction,† Research Institute of Microbial Diseases, Osaka University, Osaka; and the Department of Physiology and Cell Biology,‡ Kobe University, Kobe, Japan*

The cutaneous lymphatic system plays a major role in tissue fluid homeostasis and inflammation of the skin. Although several lymphangiogenic factors are known to be involved in the formation of lymphatic vessels, the molecular mechanisms that maintain lymphatic integrity and control the functional drainage of interstitial fluid and resolution of inflammation remain unknown. Here we show that angiopoietin-1 (Ang1) enhances lymphatic integrity and function during inflammation. Ang1 transgenic mice under the control of keratin-14 (K14-Ang1) showed attenuated edema formation and inflammation after UV B (UVB) exposure. After UVB irradiation, blood vascular permeability was inhibited in K14-Ang1 mice compared with wild-type (WT) mice. Moreover, lymphatic vessels of WT mice were markedly enlarged and leaky in inflamed skin, whereas K14-Ang1 mice showed relatively contracted lymphatic vessels together with enhanced lymphatic vascularization. Expression of endothelial-specific tight junction molecules claudin-5 and zonula occludens protein 1 (ZO-1) was strongly down-regulated in the inflamed lymphatic vessels of UVB-exposed WT mice, whereas down-regulation of both claudin-5 and ZO-1 was blocked in UVB-exposed K14-Ang1 mice. *In vitro* studies revealed that the stability of lymphatic endothelial cells was enhanced in the presence of Ang1, presumably via up-regulation of claudin-5, as well as ZO-1. Claudin-5 knockdown markedly increased the permeability of lymphatic endothelial cells. Overall, our data strongly support the idea that Ang1/Tie2 signaling promotes lymphatic integrity by modulating tight junction molecule expression during inflammation. *(Am J Pathol 2012, 180:1273–1282; DOI: 10.1016/j.ajpath.2011.11.008)*

The lymphatic vascular system, which is composed of a dense network of thin-walled capillaries in peripheral tissues such as skin, plays a major role in the maintenance of tissue fluid homeostasis, and its impairment leads to lymphedema.[1,2] Another important aspect of lymphatic function is the afferent phase of immune response. Because lymphatic vessels are the conduit not only for excess water and macromolecules, but also for inflammatory cells such as macrophages, a detailed understanding of lymphatic function could lead to the development of methods to improve the resolution of inflammation. Indeed, recent findings in mouse models have indicated that the lymphatic vasculature is actively involved in inflammatory processes.[2–4]

Several lymphangiogenic factors, including vascular endothelial growth factor (VEGF)-C/-D/-A, platelet-derived growth factor–BB, angiopoietins, and hepatocyte growth factor (HGF), are known.[1,5] It has been shown that inflammation is attenuated in VEGF-C transgenic mice, or by subcutaneous delivery of VEGF-C, as a result of skin lymphangiogenesis, which promotes lymphatic function.[4,6] In contrast, adenoviral or transgenic delivery of VEGF-A induced the appearance of giant and functionally abnormal lymphatic vessels.[7] Systematic blockade of VEGF-A markedly reduced cutaneous photosensitivity and inflammation through inhibition of the enlargement of lymphatic vessels.[8] We also found that leaky and hyperpermeable inflamed lymphatics were associated with up-regulation of VEGF-A as well as down-regulation of VEGF-C.[6,8] Together, these data suggest that lymphangiogenic factors are actively involved in inflammation by mediating structural alteration of the lymphatics. Thus, application of other lymphangiogenic factors, which may directly regulate and/or cooperatively induce functional lymphangiogenesis in inflamed tissue, may have potential as a new strategy to accelerate the resolution of inflammation.

It recently was established that angiopoietin-1 (Ang1) promotes lymphatic vessel formation.[9,10] However, in

Accepted for publication November 14, 2011.

K.K. and H.K. contributed equally to this work.

Address reprint requests to Kentaro Kajiya, Ph.D., Shiseido Innovative Science Research Center, 2-12-1 Fukuura Kanazawa-ku, Yokohama 236-8643, Japan. E-mail: kentaro.kajiya@to.shiseido.co.jp.

contrast to the detailed understanding of the role of Ang1/Tie2 signaling in migration, permeability, and inflammation of blood vascular endothelial cells,[11] it remains unknown how lymphatic function is regulated by Ang1/Tie2 signaling. Structurally, lymphatic endothelial cells possess finely arranged, but unusual and discontinuous, junctions, consisting of adherens junctions, endothelial adhesion molecules, and tight junction proteins (TJPs) such as claudins, which allow the recirculation of fluid and cells transported to peripheral tissues via blood vessels.[12] It has been reported that claudin-5 knockout mice have increased permeability of the blood-brain barrier,[13] but the role of claudin-5 in lymphatic function is completely unknown. Here, we investigated how lymphatic function is modulated in angiopoietin-1 transgenic mice under the control of keratin 14 (K14-Ang1), to obtain insight into the molecular regulation of inflammation. Our results indicate that it may be feasible to treat edema and inflammation by the induction of functional lymphangiogenesis with Ang1.

Materials and Methods

Animals

Ten female WT mice and 10 K14-Ang1 transgenic mice[14] (kindly provided by Dr. George Yanconpoulous) at 8 to 15 weeks of age were exposed to a single dose of 200 mJ/cm^2 UV B (UVB) irradiation, using 10 Toshiba FL-20 SE fluorescent lamps (Toshiba, Tokyo, Japan) that deliver energy in the UVB wavelength range (280 to 340 nm, with a maximum at 305 nm).[15] Ten female WT and 10 K14-Ang1 mice without UVB irradiation also were used as controls. The thickness of the ears was measured every day until day 3 after irradiation. Three days after the UVB irradiation, the ears were removed, embedded in OCT compound, and processed for histologic analyses. All procedures, including measurement of ear thickness and UVB irradiation, were performed under anesthesia. All animal studies were approved by the Shiseido Research Center Committee on Research Animal Care.

Plasma Extravasation and Intravital Lymphangiography

To determine the blood vascular permeability, a Miles assay was performed as previously described.[16] Briefly, mice were anesthetized and intravenously injected with 150 μL of a 1% solution of Evans Blue dye in 0.9% NaCl. At 40 minutes after the dye injection, pictures of the ears were taken and the ears were removed. The dye was eluted from the dissected samples with formamide at 56°C, and the optical density was measured by spectrophotometry (Biotrak II; GE Healthcare, Fairfield, CT) at 620 nm. An intravital lymphatic permeability assay was conducted as described.[8] A 1-μL aliquot of a 1% solution of Evans Blue dye was injected intradermally at the inner surface of the rim of the ear, using a 10-μL Hamilton syringe, to visualize lymphatic vessels. The ear was photographed at 1, 5, and 10 minutes after dye injection.

Immunostaining

Immunofluorescence analysis was performed on 6-μm cryostat sections of mouse skins, using rat monoclonal antibodies against mouse LYVE-1 (MBL, Nagoya, Japan), against mouse Ki-67 antigen (DAKO Cytomation, Glostrup, Denmark), against mouse CD11b (BD Bioscience, Bedford, CA), and against mouse panendothelial cell antigen (clone: MECA-32; BD Bioscience), a hamster monoclonal antibody against mouse podoplanin (Angiobio, Del Mar, CA), and polyclonal antibodies against mouse LYVE-1 (RELIA Tech, Wolfenbuttel, Germany), against human claudin-5 (Santa Cruz Biotechnology, Santa Cruz, CA), against human zonula occludens protein 1 (ZO-1) (Invitrogen, Carlsbad, CA), and against mouse Prox1 (Covance, Emeryville, CA). Corresponding secondary antibodies labeled with AlexaFluor488 or AlexaFluor594 (Molecular Probes, Eugene, OR) were used. Routine H&E staining also was performed. Sections were examined with an Olympus AX80T microscope (Olympus, Tokyo, Japan) and images were captured with a DP controller digital camera (Olympus). Whole-ear skin was stained with monoclonal antibodies against CD31 (clone: MEC-13.3; BD Bioscience) and against podoplanin (Angiobio) and a polyclonal antibody against claudin-5 (Santa Cruz Biotechnology). Confocal microscopic examination of whole skin was performed using a LSM5 (Carl Zeiss, Thornwood, NY), and images were processed further using IMARIS (Carl Zeiss). Morphometric analyses were performed using IP-LAB software (Snanalytics, Fairfax, VA) as described.[17] Three different fields of each section were examined and the number of vessels per square micrometer, the average vessel size, and the relative tissue area occupied by lymphatic vessels were determined in an area of the dermis within a 200-μm distance from the epidermal-dermal junction. The unpaired Student's *t*-test was used to analyze differences in microvessel density and size.

Cells

Human dermal lymphatic endothelial cells (LECs) were isolated from neonatal human foreskins by immunomagnetic purification as described.[18] Lineage-specific differentiation was confirmed by means of real-time RT-PCR for the lymphatic vascular markers Prox1, LYVE-1, and podoplanin, and for the blood vascular endothelial markers VEGF receptor-1 and VEGF-C, as well as by immunostaining for CD31, Prox1, and podoplanin as described.[19] Cells were cultured in endothelial basal medium (EBM) 2 (Lonza, Basel, Switzerland) with supplements, for up to 11 passages.

Immunoblotting and Quantitative Real-Time RT-PCR

Western blot analyses of Tie1, Tie2, ZO-1, and claudin-5 were performed as described.[19] Briefly, confluent LECs were homogenized in lysis buffer, and protein concentrations were determined using the BCA-Kit (Pierce Biotech-

nology, Rockford, IL). LECs also were treated with 500 ng/mL Ang1 for 4 hours for the detection of claudin-5 and ZO-1, or for 10 minutes for the detection of phosphorylated Tie2 and Tie2. Equal amounts of lysates (100 μg protein) were immunoprecipitated with a rabbit polyclonal antibody against Tie1 or Tie2 (Santa Cruz Biotechnology) and then immunoblotted with a rabbit polyclonal antibody against Tie1, Tie2 (Santa Cruz Biotechnology), or phospho-Tie2 (Cell Signaling, Danvers, MA). In other experiments, equal amounts of lysates (5 μg protein) were immunoblotted with rabbit polyclonal antibody against Tie1, Tie2, claudin-5 (Santa Cruz Biotechnology), or ZO-1 (Invitrogen). Specific binding was detected by means of the enhanced chemiluminescence system (Amersham Biosciences, Piscataway, NJ). Equal loading was confirmed with an antibody against β-actin (Sigma, St. Louis, MO). In addition, total RNA was isolated from LECs cultured in the presence or absence of Ang1 (10 to 100 ng) for 4 hours after serum starvation. The expression of claudin-5 mRNA was examined by quantitative real-time RT-PCR, using the ABI Prism 7000 Sequence Detection System (Applied Biosystems, Foster City, CA). The probes and primers for claudin-5 and Tie2 were predesigned by Applied Biosystems (assay IDs: Hs00533949_m1 and Hs00176096_m1, respectively). Expression levels were normalized with respect to β-actin as an internal control (forward primer: 5′-TCACCGAGCGCGGCT-3′, reverse primer: 5′-TAATGTCACGCACGATTTCCC-3′) and probe (5′-FAM-CAGCTTCACCACCACGGCCGAG -TAMRA-3′).

siRNA Transfection

Small interfering RNA (siRNA) transfection was performed using the Basic Nucleofactor Kit for primary mammalian endothelial cells (Amaxa Biosystems, Cologne, Germany) as described.[20] Briefly, after trypsinization, LECs (5×10^5) were resuspended in 100 μL of basic nucleofactor solution. Cells were transfected by electroporation (Nucleofactor II; Amaxa Biosystems), using 2.0 μg siRNA containing two different double-stranded oligonucleotides for Tie1, Tie2, claudin-5, or control siRNA. The following siRNAs were used: Tie2: 5′-GGUGCCAUGGACUUGAUCUdTdT-3′ and 5′-GGCUAGUAAGAUCAAUGGUdTdT-3′, Tie1: 5′-GGUGACACCGCUGUACUUUdTdT-3′ and 5′-GGUUACUUGUAUAUCGCUAdTdT-3′, claudin-5: 5′-GGCUAAGAAUCUGCUUAGUdTdT-3′ and 5′-CGGAAUGAAGUUUCCUUUU-3′. Control siRNA (silencer negative control #1 siRNA; Ambion, Cambridgeshire, UK) comprised a 19-bp scrambled sequence with 3′dT overhangs, having no significant sequence homology to any known gene sequence. At 72 hours after transfection, cells were used for immunoblotting or assays. Efficient knockdown of these genes was confirmed by immunoblotting.

Migration, Cord Formation, and Permeability Assays

Haptotactic cell migration of LECs was studied as described,[19] using 24-well FluoroBlok inserts of 8-μm pore size (Falcon, Franklin Lakes, NJ). Briefly, the bottom sides of the inserts were coated with 10 μg/mL fibronec-

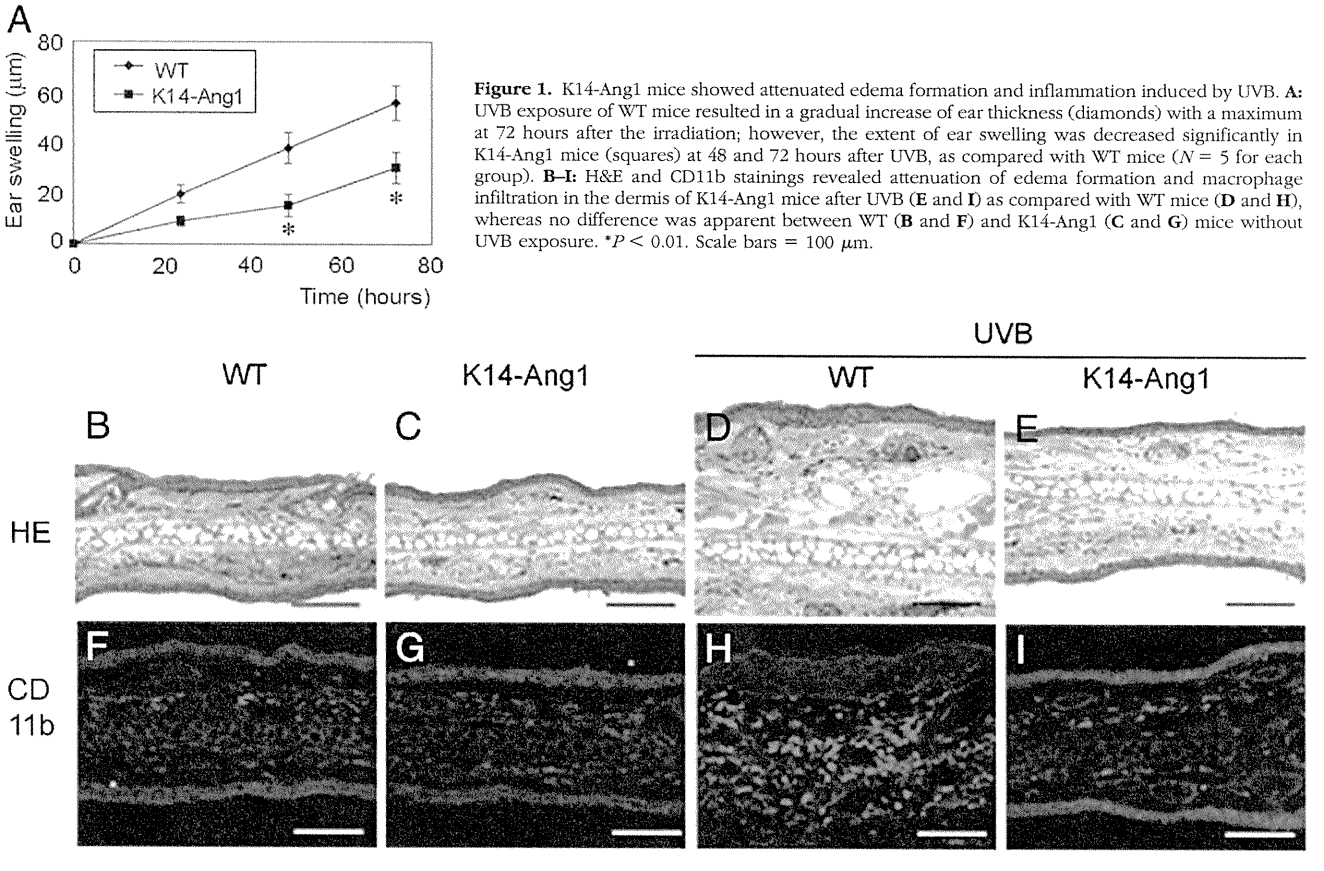

Figure 1. K14-Ang1 mice showed attenuated edema formation and inflammation induced by UVB. **A:** UVB exposure of WT mice resulted in a gradual increase of ear thickness (diamonds) with a maximum at 72 hours after the irradiation; however, the extent of ear swelling was decreased significantly in K14-Ang1 mice (squares) at 48 and 72 hours after UVB, as compared with WT mice ($N = 5$ for each group). **B–I:** H&E and CD11b stainings revealed attenuation of edema formation and macrophage infiltration in the dermis of K14-Ang1 mice after UVB (**E** and **I**) as compared with WT mice (**D** and **H**), whereas no difference was apparent between WT (**B** and **F**) and K14-Ang1 (**C** and **G**) mice without UVB exposure. $^*P < 0.01$. Scale bars = 100 μm.

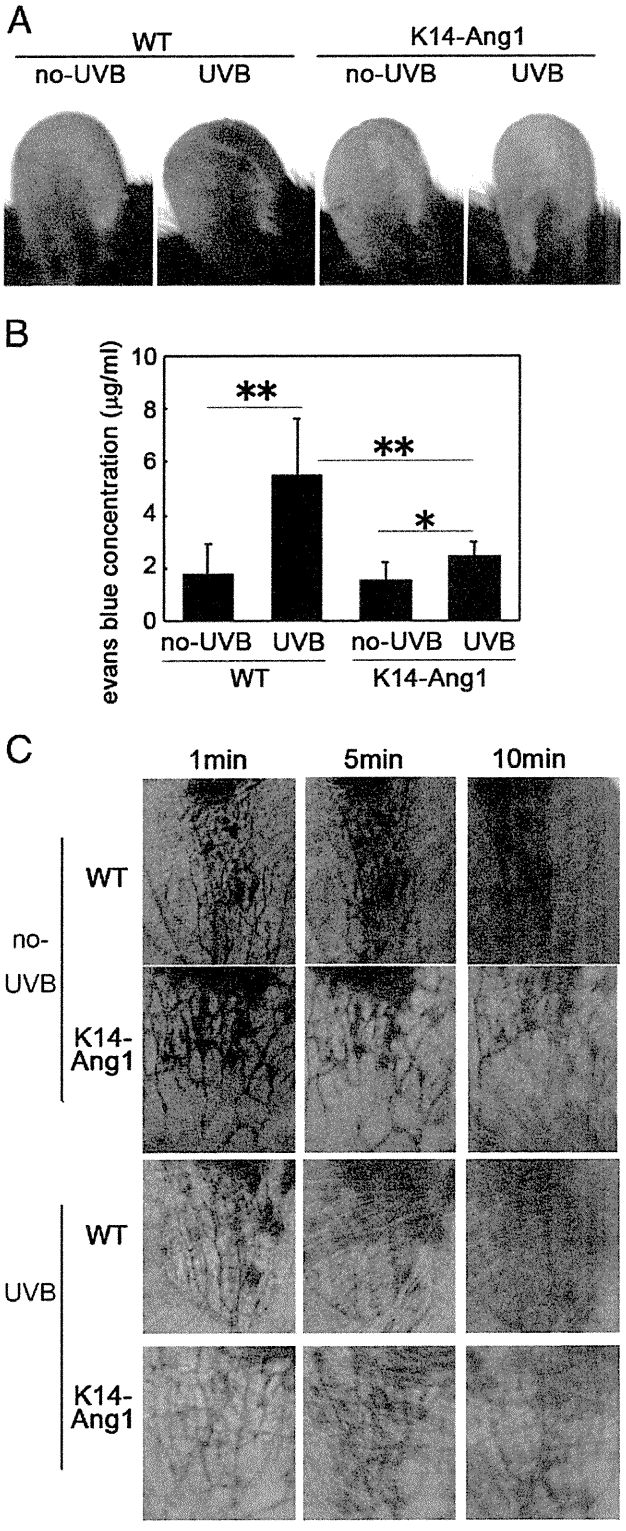

Figure 2. Decreased hyperpermeability of blood vessels as well as lymphatic vessels in K14-Ang1 mice during inflammation. **A:** The Miles assay revealed that UVB exposure induced vascular hyperpermeability of WT mice, whereas this effect was inhibited markedly in K14-Ang1 mice, as compared with WT. **B:** Quantitative analysis showed increased Evans blue leakage in the ear of UVB-irradiated WT mice as compared with UVB-irradiated K14-Ang1 mice ($N = 3$ for each group). **C:** Intravital lymphangiography revealed that lymph leakage was apparent in the whole ear of UVB-exposed WT mice at 5 and 10 minutes after dye injection, whereas the leakage was attenuated markedly in K14-Ang1 mice as compared with WT. Without UVB, there was no significant difference of lymph leakage at 5 minutes, however, at 10 minutes K14-Ang1 mice showed inhibited dye leakage. $^{*}P < 0.05$, $^{**}P < 0.01$.

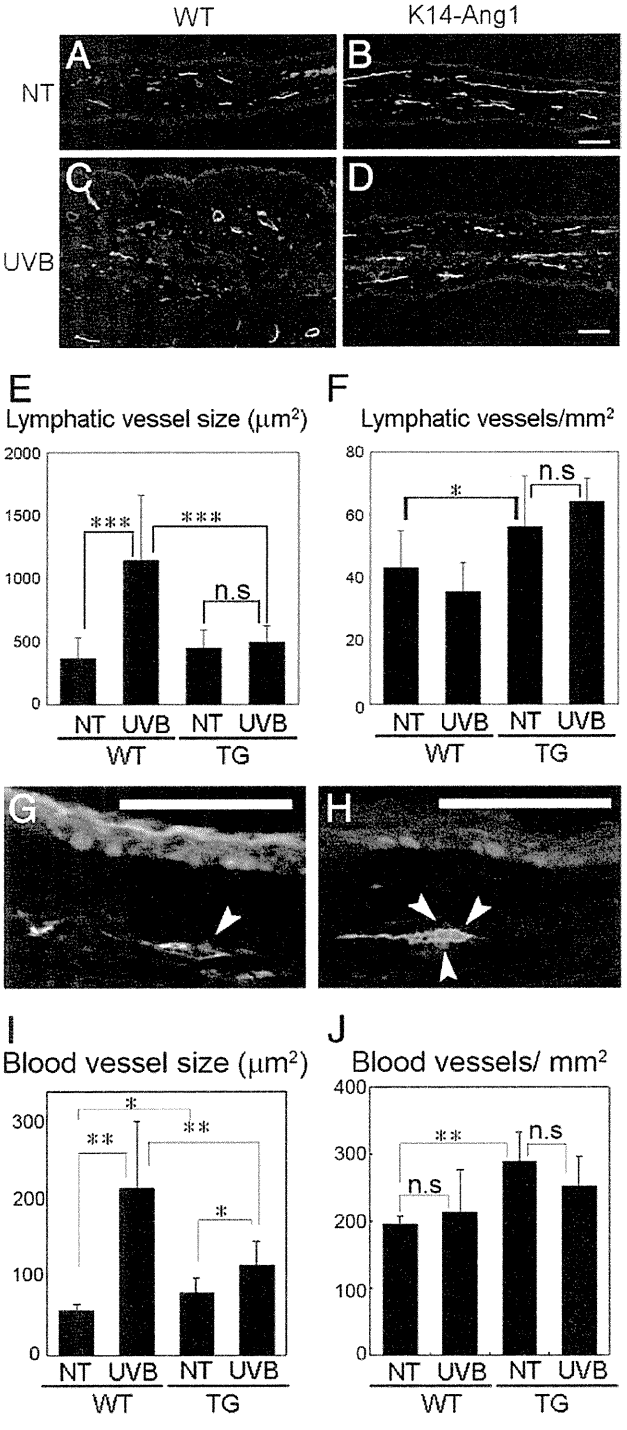

Figure 3. Inhibited enlargement of lymphatic vessels in inflamed K14-Ang1 mice. **A–D:** Double-immunofluorescence analysis using antibodies for blood vessel–specific antigen, panendothelial antigen-1 (red), and LYVE-1 (green) revealed marked enlargement of LYVE-1–positive lymphatic vessels in UVB-exposed WT mice (**C**) as compared with ear skin not exposed to UVB (non-UV) (**A**), whereas in K14-Ang1 mice, the enlargement of lymphatic vessels after UVB exposure was attenuated (**D**). In contrast, more lymphatic vessels were found in K14-Ang1 mice (**B**), as compared with WT mice (**D**). **E** and **F:** Morphometric analysis using ear sections stained with LYVE-1 showed pronounced enlargement of lymphatic vessels of WT mice after UVB irradiation, whereas the lymphatic enlargement was strongly inhibited in K14-Ang1 mice (**E**). The density of lymphatic vessels was increased in K14-Ang1 mice, as compared with WT mice (**F**). **G** and **H:** Double-immunofluorescence analysis for proliferation marker Ki-67 (red) and podoplanin (green) showed greater proliferation of lymphatic endothelial cells in K14-Ang1 mice (**H, arrowheads**) as compared with WT mice (**G, arrowheads**). **I** and **J:** Under physiological conditions, the size (**I**) and density (**J**) of blood vessels were increased in K14-Ang1 mice. After UVB irradiation, the change of blood vessel size was smaller in K14-Ang1 mice than in WT mice. The density was comparable in skins exposed and not exposed to UVB ($N =$ 5 for each group). $^{*}P < 0.05$, $^{**}P < 0.01$, and $^{***}P < 0.001$. Scale bars = 100 μm.

tin (BD Bioscience) for 1 hour. LECs (100 μL; 1 $\times$ 10^6 cells/mL) in serum-free EBM were seeded into the upper chambers and incubated for 4 hours at 37°C in the presence of Ang1 (5 to 500 μg/mL). The fluorescence intensity (proportional to the number of viable cells) was measured using a Fluoroskan Ascent (Thermo Fisher Scientific, Waltham, MA). Cord-formation assays were performed as described.[19] LECs after transfection of either Tie1, Tie2, or control siRNA were grown on fibronectin-coated 24-well plates until confluence. Then, 0.5 mL of a neutralized isotonic bovine dermal collagen type I solution (Vitrogen, Palo Alto, CA) with or without Ang1 (500 ng/mL) was added to the cells. After incubation at 37°C for 6 hours, cells were fixed with 4% paraformaldehyde for 30 minutes at 4°C. Representative images were captured and the total length of tube-like structures per area was measured using the IP-LAB software, as described.[19] A permeability assay also was performed. Briefly, LECs were grown to confluence on the fibronectin-coated surface of 0.4-μm pore size tissue culture inserts (Corning, Lowell, MA), followed by culture in serum-free EBM for 24 hours. Then, the upper and lower chambers were cultured in the presence or absence of angiopoetin-1 (50 to 500 ng/mL) together with S-nitroso-N-acetylpenicillamine[20](Sigma) for 6 hours. fluorescein isothiocyanate–dextran was added to the upper chambers, and after incubation for 15 minutes the concentration of fluorescein isothiocyanate–dextran in the lower chambers was determined at 492 nm using a Fluoroskan Ascent spectrophotometer (Thermo Fisher Scientific).

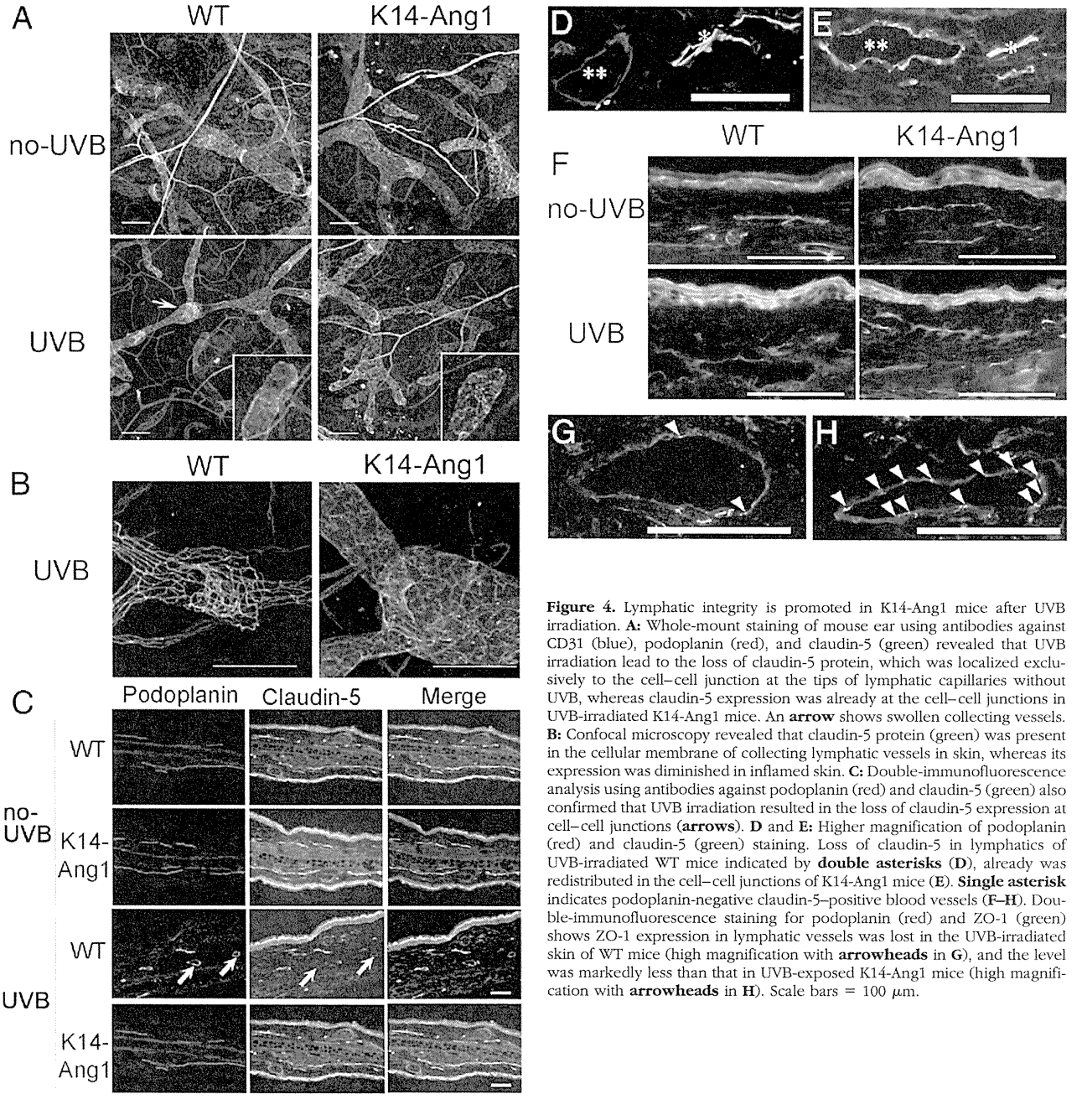

Figure 4. Lymphatic integrity is promoted in K14-Ang1 mice after UVB irradiation. **A:** Whole-mount staining of mouse ear using antibodies against CD31 (blue), podoplanin (red), and claudin-5 (green) revealed that UVB irradiation lead to the loss of claudin-5 protein, which was localized exclusively to the cell–cell junction at the tips of lymphatic capillaries without UVB, whereas claudin-5 expression was already at the cell–cell junctions in UVB-irradiated K14-Ang1 mice. An **arrow** shows swollen collecting vessels. **B:** Confocal microscopy revealed that claudin-5 protein (green) was present in the cellular membrane of collecting lymphatic vessels in skin, whereas its expression was diminished in inflamed skin. **C:** Double-immunofluorescence analysis using antibodies against podoplanin (red) and claudin-5 (green) also confirmed that UVB irradiation resulted in the loss of claudin-5 expression at cell–cell junctions (**arrows**). **D** and **E:** Higher magnification of podoplanin (red) and claudin-5 (green) staining. Loss of claudin-5 in lymphatics of UVB-irradiated WT mice indicated by **double asterisks** (**D**), already was redistributed in the cell–cell junctions of K14-Ang1 mice (**E**). **Single asterisk** indicates podoplanin-negative claudin-5–positive blood vessels (**F–H**). Double-immunofluorescence staining for podoplanin (red) and ZO-1 (green) shows ZO-1 expression in lymphatic vessels was lost in the UVB-irradiated skin of WT mice (high magnification with **arrowheads** in **G**), and the level was markedly less than that in UVB-exposed K14-Ang1 mice (high magnification with **arrowheads** in **H**). Scale bars = 100 μm.